

JRD

Jordan River Dureijat (JRD)

2017 Excavation Report



Excavation Permit Number – G/68-2016

Submitted to the Israel Antiquity Authority
April 2018

Gonen Sharon, Elizabeth Bunin, Daniella E. Bar-Yosef Mayer,
Natalie D. Munro and Steffen Mischke

The JRD Excavation Project is supported by:

The Israel Science Foundation

The Wenner-Gren Foundation

National Geographic Foundation

Curtiss T. & Mary G. Brennan Foundation for Archaeological Research

The CARE Foundation

Tel Hai College Research Grants



INTRODUCTION.....	3
2017 Geological Core Drilling.....	5
Core data:	7
Core JRD-1 2017.....	7
Core JRD-2 2017.....	8
Core scanning and analysis	10
JRD Excavation 2017 – updated Stratigraphy and Chronology.....	13
Site Stratigraphy at the end of 2017 season.....	13
Deep Sounding	17
O-96 Sounding	17
Q-99 sounding.....	23
JRD Radiocarbon Dating and Age Modeling.....	24
JRD 2017 EXCAVATION SEASON	29
Excavation methodology	29
Area B Northern Squares - Layer 3a & 3b Natufian.....	30
Upper Natufian Layers - Layer 3a.....	30
Layer 3c.....	46
Layer 4.....	46
Below Layer 4	48
Layer 5.....	50
Site preservation and closing.....	58
Directions for future excavations	60
References	61
Appendix 1	63
Appendix 2	64

INTRODUCTION

The site of JRD was discovered during the massive drainage operation of the Jordan River in December 1999 (Marder et al., 2015; Sharon et al., 2002a; Sharon et al., 2002b). The site was first observed in piles of sediment on the banks of the river some 1300m north of the Benot Ya'aqov Bridge (Fig.1c) and finds were collected from the piles on the east bank. In the summer of 2002, a survey was conducted to evaluate the damage of the drainage operation. During this survey, a test excavation of one square meter (Section 6-02) was dug on the east bank of the Jordan River. A full account of the results of the 2002 survey and test excavation was published (Marder et al., 2015). Please refer to this publication for details and data regarding past research at the site. For a description of the 2014 test excavation season at JRD please refer to the 2014 report submitted to the IAA June 2015. For details and data regarding the 2015 and 2016 excavation seasons please refer to the reports submitted to the IAA (Fig. 2).

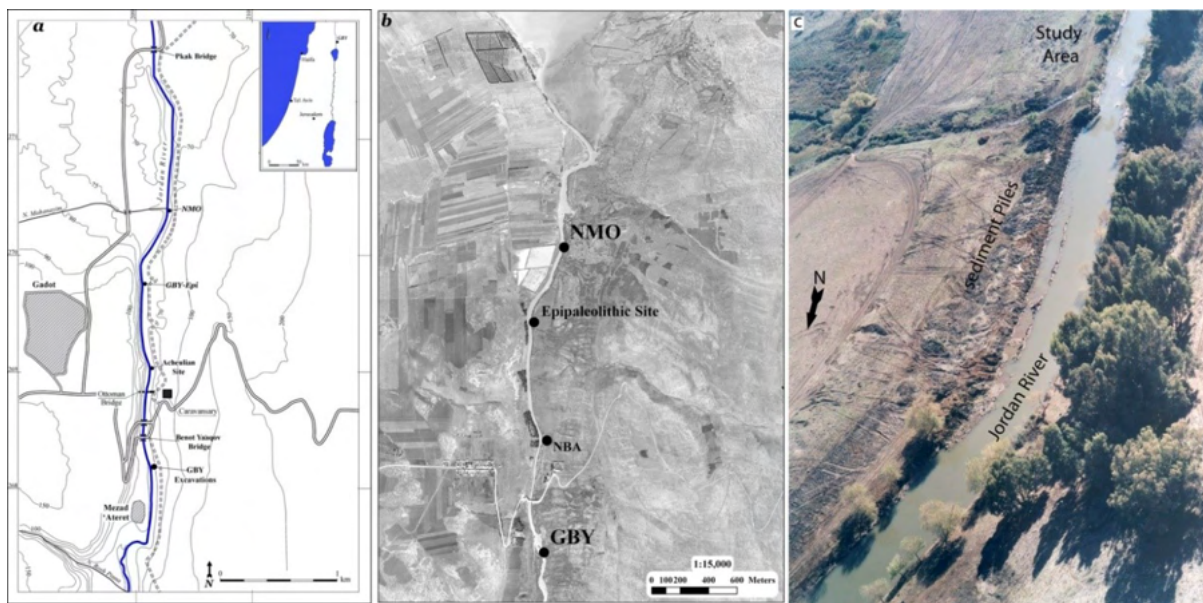


Figure 1: a. JRD location map; b. location of prehistoric sites on 1945 aerial photo; and c. view of the site during drainage work in 1999.

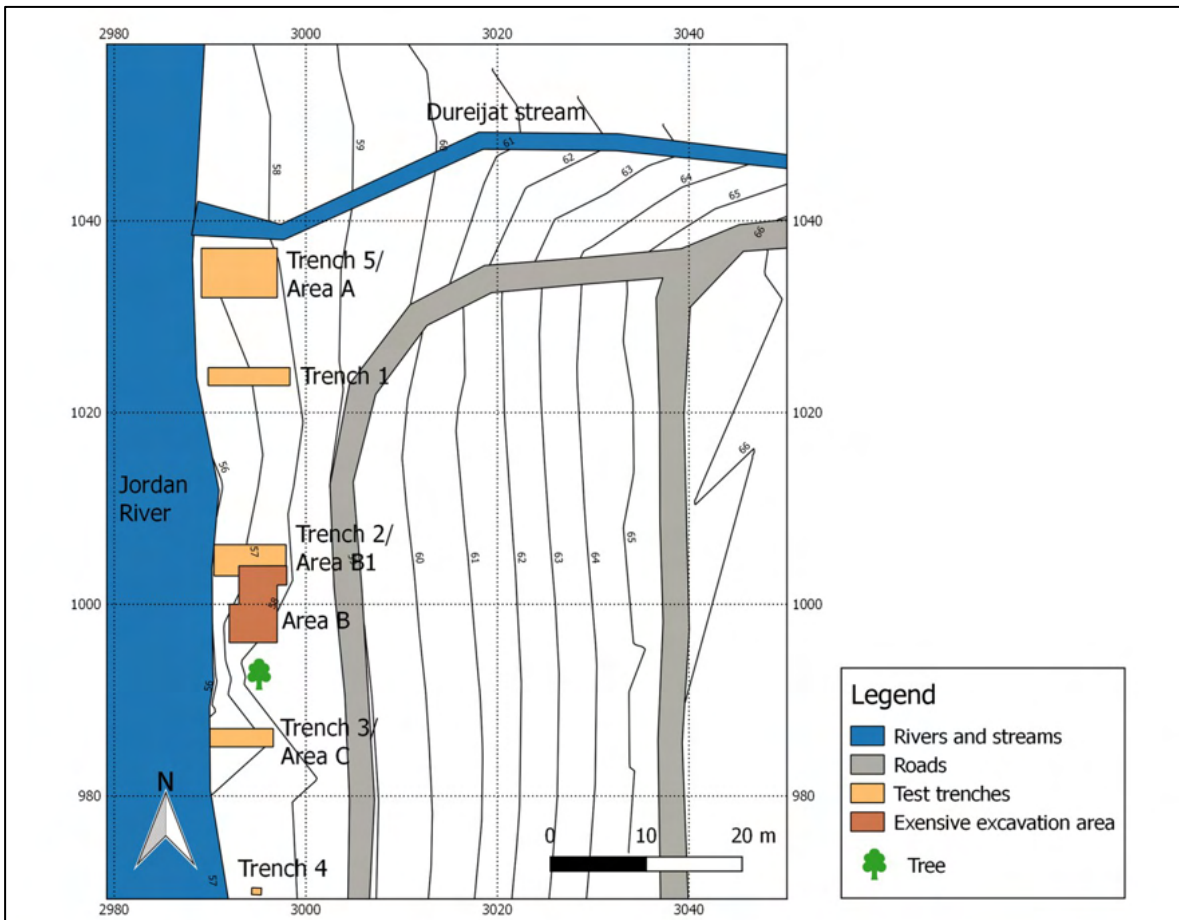


Figure 2: JRD plan and Area B at the end of the 2017 season.

2017 Geological Core Drilling

In order to extend the length of the JRD geological sequence, a geological core was extracted at the site. Core drilling took place on May 8, 2017 (Figs. 3, 4). At first, an unlined core of 3" diameter (6cm) was drilled at square R-98 of the site's grid. Drilling using water injection to cool the drill bit turned out to be problematic when drilling the soft, muddy sediments of JRD. Core HULA-JRD17-1A was drilled to a depth of 13.90m but recovery rate was low (see core log below & Fig. 5). This led to the decision to move the location of the core 10m northward. Core HULA-JRD17-1B was much more successful with better recovery rate and drilled to a depth of 24.5m. The core lithology and section are presented in the log & Fig. 6. The sediments extracted were documented in the field and wrapped in plastic to preserve moisture of the sediments. The cores are housed at Dr. Nicolas Waldman's lab at the Department of Marine Geosciences, Haifa University.



Figure 3: Drilling machine crossing the Dureijat stream on its way to JRD



Figure 4: Geological core drilling

Core data:

Core JRD-1 2017

Core description

Project Name	PointID	East	North	Hole Depth	Elevation	GW Depth	Drill Type	Date Started	Date Finished	Drilling Contractor	Supervised By
	'Borehole	X (m)	Y (m)	Total Depth (m)	(m)	(m)					
Dureijat	JRD-1	769882	259060	13.90			HQ 3"	08.05.17	08.05.17	Geosampler	Sharon.R-GaiaLog, Geoprospect

Core log:

PointID	Depth	Depth to base	General description	Recovery (%)	RQD (%)	Core #	box	Water Loss or Return
JRD-1	0.00	1.50	No recovery (upper part; silt and sand, brown, mostly fine to medium grain size, sub angular, with shell fragments).	0	0	1	BOX 1 (0.0-11.40)	WR
JRD-1	1.50	3.15	Silt with fine sand, dark brown, high to medium plasticity (upper part; 5cm gray basalts).	51		2		WR
JRD-1	3.15	4.95	Silt, dark gray, high to medium plasticity, with fine sand and fines/clay, with some fine gravel and shell fragments, organic matter smell.	67		3		WL
JRD-1	4.95	6.00	As above; gravel up to 1.5cm, sub angular.	100		4		WL
JRD-1	6.00	6.50	No recovery.	0		5		WL
JRD-1	6.50	7.50	No recovery.	0		6		WL
JRD-1	7.50	8.50	No recovery.	0		7		drilling without water
JRD-1	8.50	9.50	No recovery.	0		8		drilling without water
JRD-1	9.50	12.10	Silt, dark gray, high to medium plasticity, with fine sand and fines/clay, with some basalt gravel up to 8cm. 11.20m: Melanopsis shells up to 2cm, with dark brownish gray silt with fine sand and fine gravel.	48		9	BOX 2 (11.40-13.9)	WL
JRD-1	12.10	13.90	No recovery.	0		10		WL

Core JRD-2 2017

Core description:

Project Name	PointID	East	North	HoleDepth	Elevation	GW Depth	Drill Type	Date Started	Date Finished	Drilling Contractor	Supervised By
	'Borehole	X (m)	Y (m)	Total Depth (m)	(m)	(m)					
Dureijat	JRD-2			24.50			HQ 3"	08.05.17	08.05.17	Geosampler	Sharon.R-GaiaLog, Geoprospect

Core log

PointID	Depth	Depth to base	General description	Recovery (%)	RQD (%)	Core #	Box	Water Loss or Return
JRD-2	0.00	1.50	Silt and sand, brown, mostly fine to medium grain size, sub angular. From 1.0m; Silt, dark gray, high to medium plasticity, with fine sand and fines/clay, with some fine gravel and shell fragments.	43		1	BOX 1 (0.0-9.30)	WL
JRD-2	1.50	3.50	As above; rich in shells, organic matter smell.	22		2		
JRD-2	3.50	4.50		18		3		
JRD-2	4.50	5.50	Silt, dark gray, high to medium plasticity, with fine sand and fines/clay, with some fine gravel and shell fragments.	23		4		Drilling without water.
JRD-2	5.50	6.50	As above; with some basalt gravel up to 6cm.	20		5		WL
JRD-2	6.50	9.50	As above; with some basalt & limestone gravel. Drilled without rotation- twisted core.	70		6		
JRD-2	9.50	12.50	Silt, dark gray, high to medium plasticity, with fine sand and fines/clay, with shell fragments and some basalt & limestone gravel up to 4cm.	19		7	BOX 2 (9.30-14.95)	
JRD-2	12.50	14.35	As above; rich in Melanopsis shells in places. 12.75m; Wood piece- 4.5cm, dark brown. 13.90m; Basalt, dark gray, strong, highly porous up to 0.5cm with calcite coating (and olivine).	92	9	8		
JRD-2	14.35	18.50	Basalt, dark gray, strong, highly porous up to 0.5cm with calcite coating (and olivine).	100	43	9		
			15.25; Limestone fragment. 15.30; Silt, dark gray, high to medium plasticity, with fine sand and fines/clay, with some gravel.	33		10	BOX 3 (14.95-22.3)	
JRD-2	18.50	21.50	Silt, light gray, high to medium plasticity, with fine sand and fines/clay, with some fine limestone gravel up to 3cm.	28		11		
JRD-2	21.50	23.20	As above; dark gray. 23.10m; Wood pieces, dark brown.	100		12		
JRD-2	23.20	24.50	Silt, light gray, high to medium plasticity, with fine sand and fines/clay, with some gravel.	54		13	BOX 4 (22.3-24.5)	

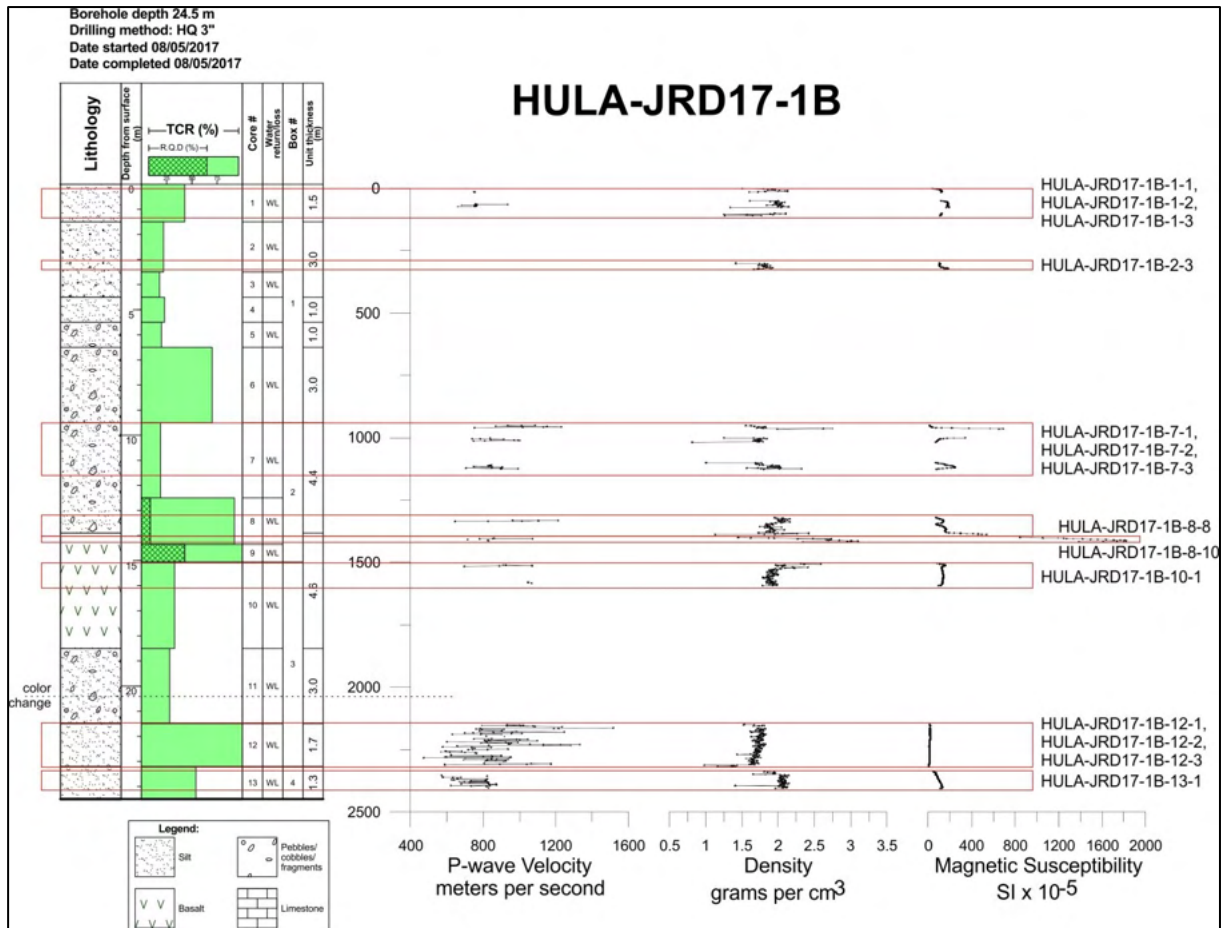


Figure 5: Core JRD-1 2017 log

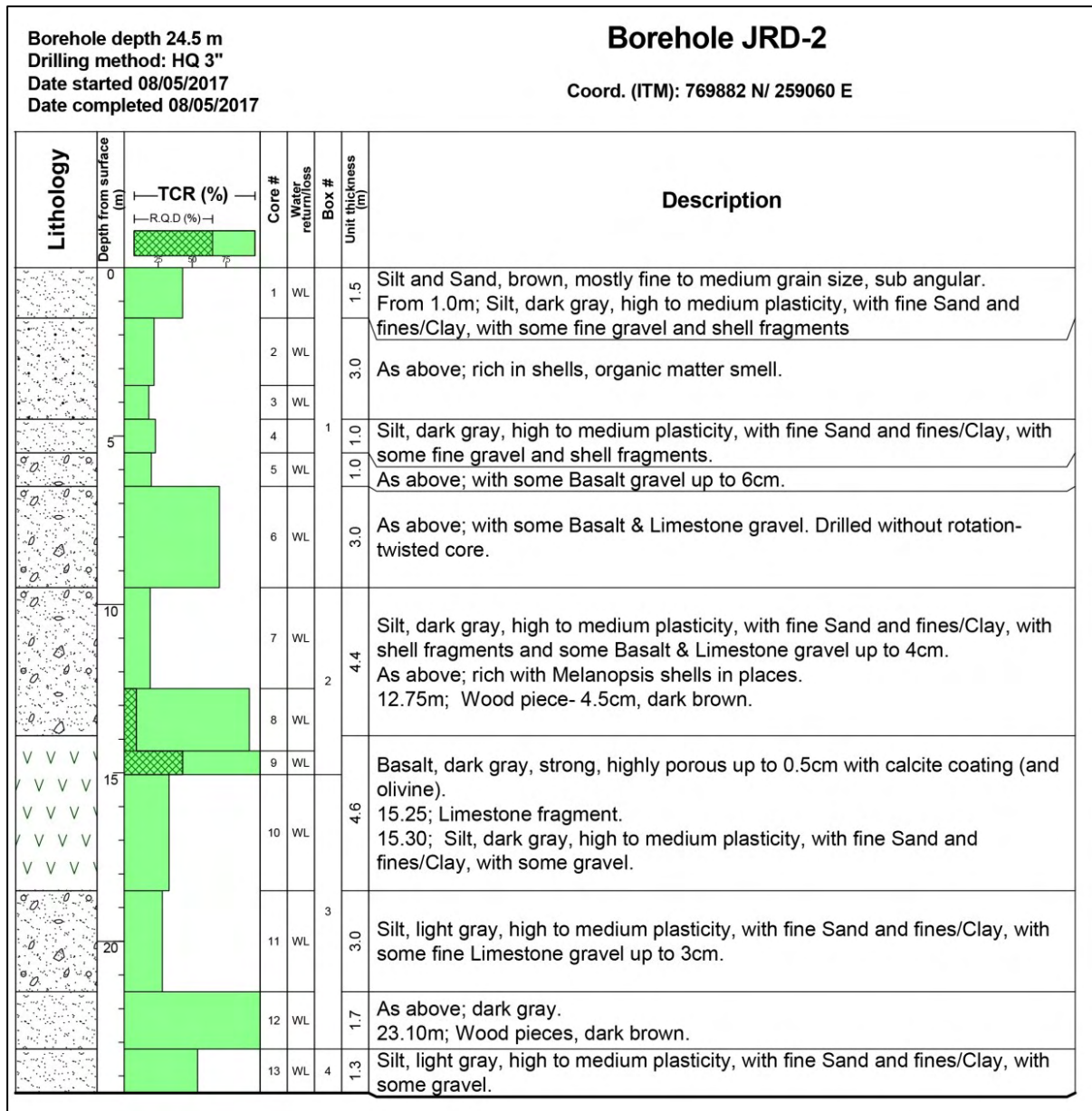


Figure 6: Core JRD-2 2017 log

Core scanning and analysis

Liz Bunin

Immediately after drilling, the cores were transported to the Haifa University - Basin Analysis and Petrophysical Laboratory directed by Dr. Nicolas Waldmann. The cores were analyzed using a multi-sensor core logger (see description at <http://marsci.haifa.ac.il/index.php/en/equipment-petro>) to measure sediment density, magnetic susceptibility, and p-wave velocity when possible. The data for the second core was plotted against the logs that Geoprospect provided (Fig. 6).

Core Splitting

Core opening took place in August at the University of Haifa; the cores were split in half lengthwise using wire and metal plates and, following the regular procedure for geological core analysis, one half has been used for sampling and analysis (“working half”) while the other half has been preserved as an archive (“archive half”). The surfaces of the work halves were cleaned (Fig. 7), described and photographed.



Figure 7: core splitting at Haifa University lab.

Core Photography

Photographs of the working halves were produced using a digital camera mounted on a tripod. Photographs were taken from directly above at intervals of 20 cm, such that we would be able to stitch them together on the computer and the photos would not appear distorted.

Core Logging and Sampling

After the cores were photographed, the cleaned split core faces were measured and described (color, shell content, sedimentology/lithology, structures and clasts, etc). The work on the complete log of the core is ongoing.

Dr. Naomi Porat (Israel Geological Survey) took samples for dating from the working halves of HULA-JRD17-1B and all of these samples start with the prefix DUR or DRJ.

- DUR1 is cm 3-11 of the working half of HULA-JRD17-1B-7-1
- DUR2 = cm 2-12 of the working half of HULA-JRD17-1B-8-1
- DRJ3 = cm 57-65 of the working half of HULA-JRD17-1B-8-8
- DRJ4 = cm 75-84 of the working half of HULA-JRD17-1B-10-1

In addition, fifteen small samples, approximately four grams each, have been collected for a preliminary assessment of the sedimentology and micropaleontology. These samples have been frozen and are being stored at Haifa University.

The results of the OSL dating were obtained in April 2018 and are presented in Table 1:

Table 1: JRD core 1 OSL results

Sample	Depth (m)	Water (%)	Dose rate ($\mu\text{Gy/a}$)	O-D (%)	N	De (Gy)	Age (ka)
DUR-1	9.6	64	856 \pm 35	10	18/18	84 \pm 3	98 \pm 5
DUR-2	12.6	55	905 \pm 39	10	20/20	88 \pm 3	97 \pm 5
DUR-3*	13.6	50	1220 \pm 53	26	9/10	101 \pm 7	83 \pm 7
DUR-4*	18.3	59	1210 \pm 49	16	14/14	159 \pm 7	132 \pm 8

Notes: Grain size for all samples 64-125 μm .

* There was very little quartz separated from these samples and only N aliquots were measured.

JRD Excavation 2017 – updated Stratigraphy and Chronology

Site Stratigraphy at the end of 2017 season

The stratigraphy of Area B was described in previous reports. The sets of shell horizons and associated underlying mud units that make up Layers 3, 4 and 5 are interpreted as reflecting deposition in an environment where the distance from the lakeshore to the study area is changing cyclically. Shell horizons in these layers are not uniformly thick throughout the excavation area, and in some places bifurcation of individual shell horizons may indicate locally higher sedimentation rates. The 2017 season in the main part of Area B focused on the lower part of the stratigraphic sequence, namely Layer 4 and below (Figs. 8 & 9). The stratigraphy of the upper layers, the upper part of layer 3 (Layers 3a and 3b) is discussed below.

During the 2017 season, the last remnants of Layer 3c were removed, primarily from the squares to the northeast of Area B – square line 101 and 100 (Fig. 10). In the other parts of Area B, the Layer 4 sequence was removed (see detailed discussion below) in an attempt to expose Layer 5 on a large scale. Figures 8 & 9 present Area B at the end of the 2017 season. Figure 10 illustrates the stratigraphic position for the squares at the end of the season.



Figure 8: JRD Area B at the end of the 2017 season from the south



Figure 9: JRD Area B at the end of the 2017 season from the north



Figure 10: JRD Area B stratigraphy at the end of the 2017 season from the north

As can be seen in Figure 10, in most of Area B Layer 4 was removed and the squares are exposed to the level called “below Layer 4”. Layer 5 was reached primarily in Line N squares. Two deep sounding pits, at Square O-96 and Q-99 have enabled us to establish the stratigraphy presented below. The general stratigraphy of Area B, as understood after the 2017 season, is presented in Figures 11 & 12. The new data added to our understanding during the 2017 season as follows:

Layer 4 is now subdivided into 3 phases/levels (a, b & C). Level 4b is the stony layer exposed in the previous seasons and is comprised primarily of basalt and limestone cobbles, with all (or most) determined to have been imported to the site as net sinkers. This level covers the entire Area B surface and is deposited on different sediments changing from dark mud at the eastern part of Area B to shell rich shore material at the western squares. See detailed discussion below. At the westernmost part of Area B, at square line M and partly N, Layer 4 is disturbed by sediments penetrating the sequence from the east, probably representing shoreline material cutting into the sequence at a later time and disturbing the stratigraphy. The M squares were observed to be so disturbed during the 2016 season that we decided not to excavate them during the 2017 season to avoid the non-primary context. Nevertheless, during the excavation of the N line squares in 2017, below Layer 4 and into the mud layer separating Layer 4c from Layer 5, it became evident that the stratigraphy becomes clearer and that layer 5 is a distinct unit of its own. It seems that Layer 5 at the western part of Area B accumulated into a depression gaining a considerable thickness (up to 20 cm and possibly more) toward the west. As a result, we excavated square M-99 and, indeed, after removing some 30 cm of mud, the top of layer 5 was unearthed. Layer 5 is rich in lithic artifacts and bones, and since it is the first layer excavated into sediment that did not dry post the 1999 drainage operation that brought the water level in the Jordan below the upper layers (Marder et al., 2015), the waterlogged layer preserved large pieces of wood (see below).

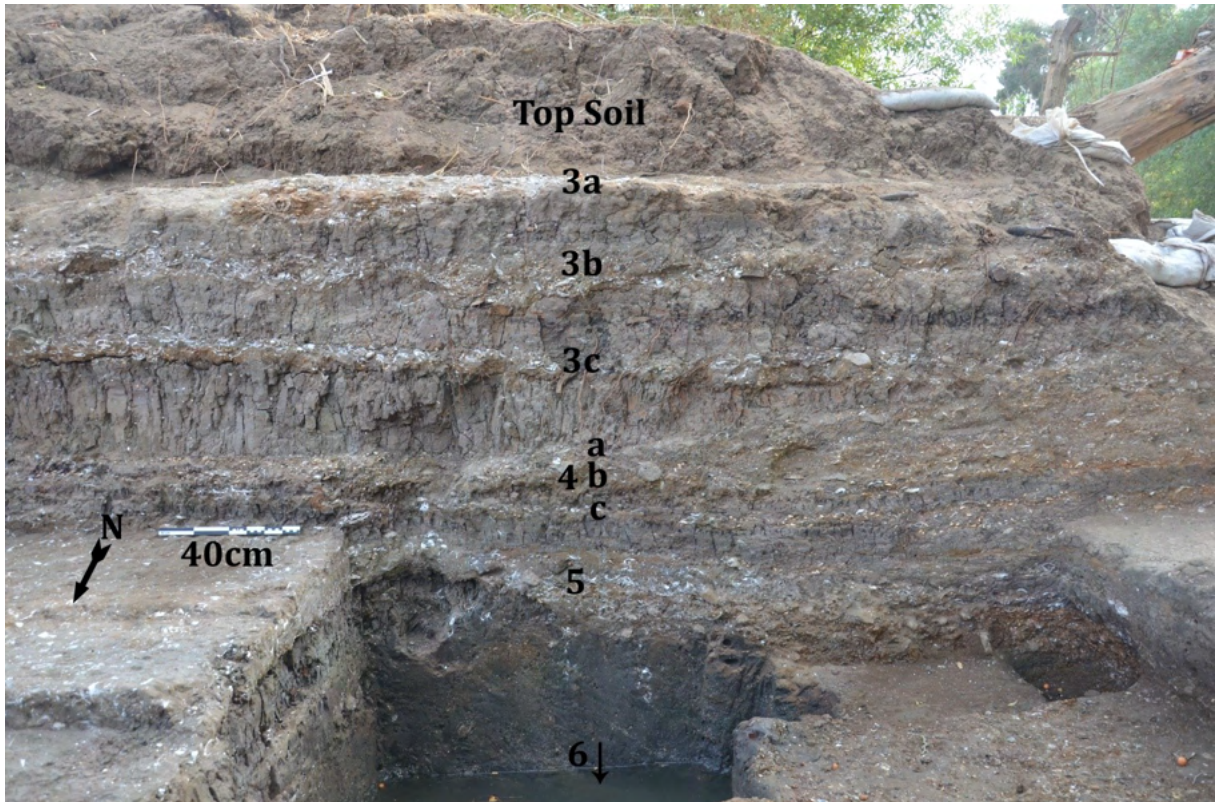


Figure 11: JRD Area B South Section stratigraphy end of 2017 season



Figure 12: JRD Area B South Section stratigraphy end of 2017 season – Layer 5 and west disturbance highlighted.

Deep Sounding

Two deep soundings were excavated into the levels below Layer 5 aiming to explore the lower stratigraphy of the site. The primary test pit one was at square O-96 where the entire square was carefully excavated. The second sounding, in square Q-99, was dug rapidly during the last two days of excavation with the goal of locating layer 6 at the eastern part of Area B (Fig. 10). Only two sub-squares were dug (the eastern ones, sub-squares c & d).

O-96 Sounding

The O-96 square was selected for deep sounding as excavation in 2016 reached the deepest point in Area B. Layer 5 was mostly excavated here. Excavation started by removing the last part of Layer 5 (Fig. 12) at level of c. 56.00 MASL. The method of excavation was identical to the site methodology except for the use of 10cm spits instead of 5 cm ones. The sequence exposed was challenging all along (Fig. 13). From the very first spit removed it became clear that the stratigraphy is complex. It seems that the layers are vertical instead of horizontal. The sediments were of very fine dark clay and mollusk-rich sand, sometimes actually made of crushed shells and in other parts of the square from mini-shells. Sediments smelled of organic remains, preservation of botanic material seems to be good but many roots (possibly recent) can be observed. A few basalt pebbles were exposed as well as rare flint and some isolated bones. Fish teeth were found as well. The molluscs and, in particular the *melanopsis*, preserve their dark color, an indication for very good preservation conditions (Fig. 14).

At a level of c. 55.60 or 55.55, it seems that we reached the water level in the Jordan River (river water level fluctuates daily, sometimes up to 20-30 cm) and water started filling the pit. This made work more challenging. Water flow into the pit is probably through the sandy layers and the flow is constant but still manageable.



Figure 13: Square o-96 deep sounding during excavation; three levels.



Figure 14: Mollusks from O-96 deep sounding. Note preservation of colors.



Figure 15: O-96 Layer 6 flint tools



Figure 16: Bone in O-96 deep sounding. Above Layer 6

At a level of 55.20, some 80 cm below Layer 5, a layer rich with basalt pebbles and cobbles and some weathered limestone was reached (Fig. 15 - 17). The matrix is of sand and numerous crushed molluscs. Numerous flint tools in good preservation state were exposed, including a massive scraper and bladelet core (Fig.15). No bones were observed and only a few botanical remains, primarily charcoal, were observed. This layer was termed Layer 6.



Figure 17: Layer 6 at square O-96

Explanation of the unclear stratigraphy exposed below Layer 5 came only when the section of deep sounding O-96 was exposed and observed by geologists (S. Mischke & N. Waldman). The section reflects a “fluid escape structure”. A layer full of water, as sand is locked between layers with low water permeability as the clay muddy layers above and below Layer 6. In time, the upper layer accumulates and gains weight, creating increasing pressure on the sealed water below. Then, a sudden event, such as an earthquake, can cause the water to erupt through a weak point (such as a small fault) to the surface, pushing the sediments of the layer up with the water. The result is an eruption like stratigraphy with near vertical position of the layers at the point of eruption, as can be seen in the south section of the O-96 Sounding (Figs. 18-21). Such an event can explain some of the differences observed in the sediments below Layer 4 between east and west parts of Area B. It also makes the context of the layers in square O-96 problematic. After observing this phenomenon at square O-96, it became clear

that samples for geological and pollen analysis should be collected from a square with better context.



Figure 18: O-96 deep sounding sections

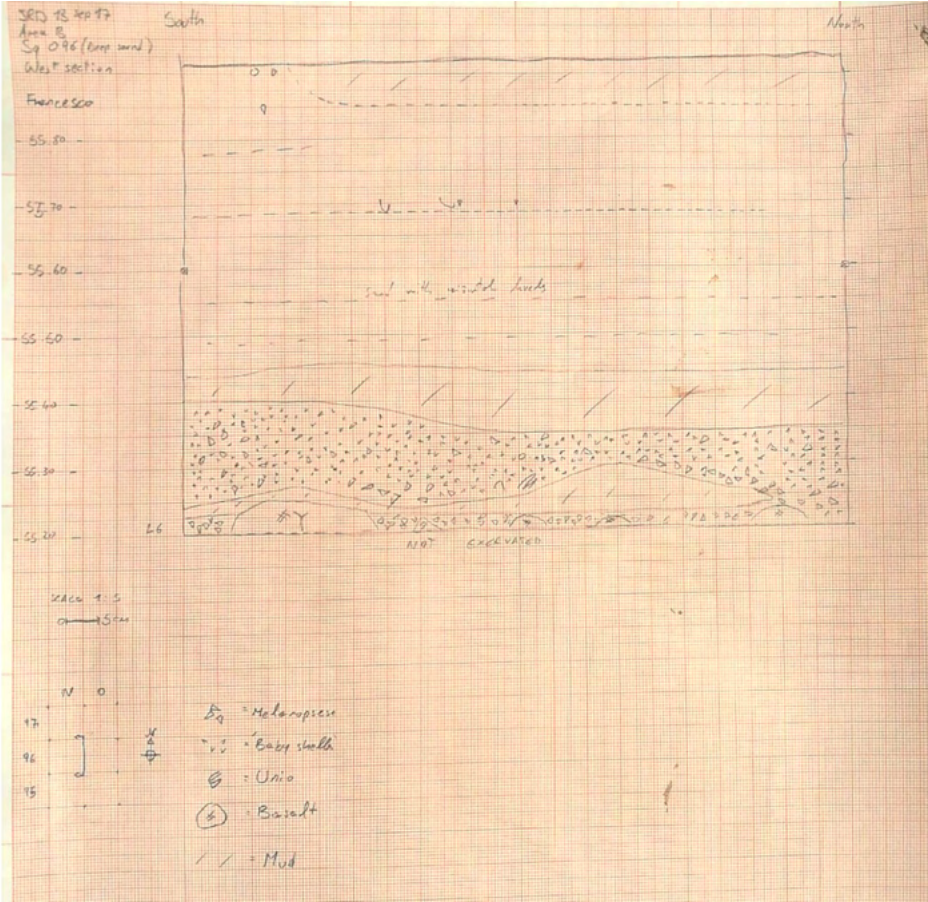


Figure 19: O-96 deep sounding west wall drawing.



Figure 20: O-96 south section



Figure 21: O-96 south section and drawing.

Q-99 sounding

The Q-99 sounding (Fig. 10 for location) was dug rapidly, during the last two days of excavation, with the goal of locating layer 6 at the eastern part of Area B. Only 2 sub-squares were dug (the eastern ones, sub-squares c & d). The stratigraphy here is completely different than the one observed in the west part of Area B. Layer 5 is probably a muddy, non-archaeological shell horizon (mostly *Unio*id) and layer 6, if indeed layer 6, was observed to be a layer of basalt, ranging in size from cobbles to small boulders (Fig. 22). No real archaeological horizons were identified along the sequence here and no finds (flint, bone or botanic) were obtained. It is suggested that the entire sequence here accumulated under water. Nevertheless, the sequence seems to be of good context and continues the upper sequence exposed at this part of the site in previous years. High resolution (1cm) geological samples were collected from this section for geochemical study as well as for pollen analysis.

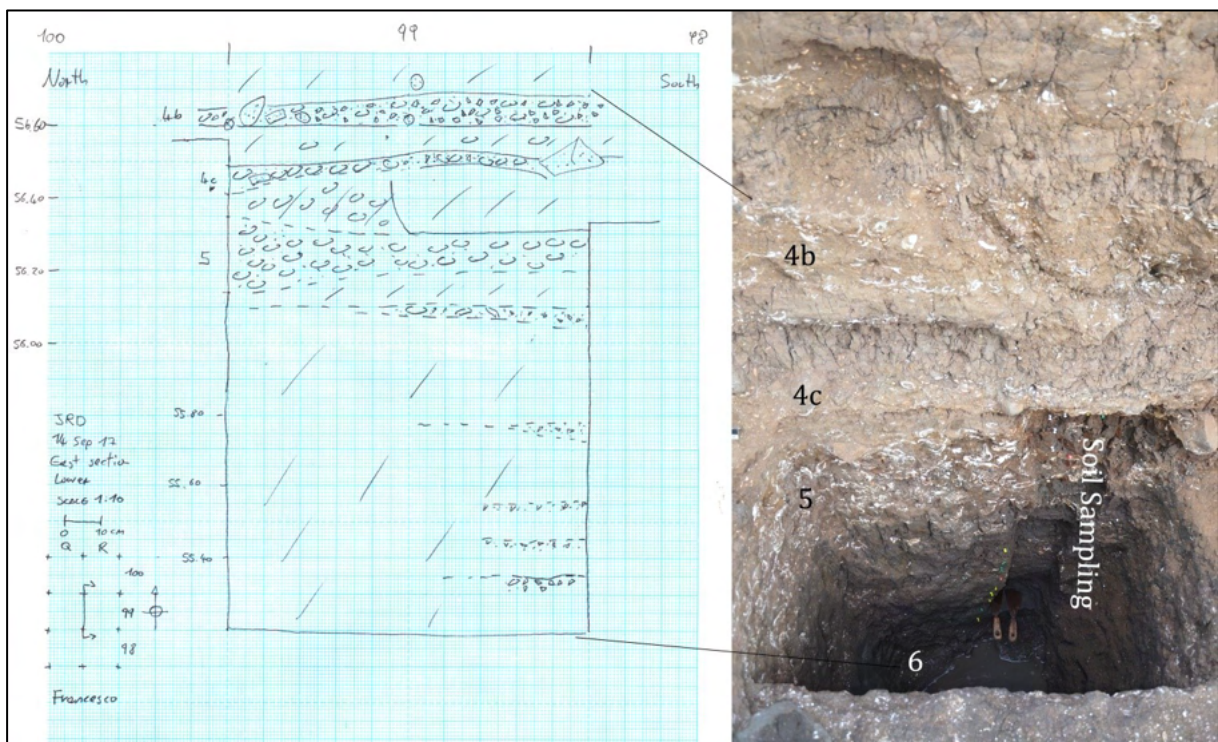


Figure 22: Q-99 Deep sounding east section

In light of this stratigraphic observation, it seems that the squares east of the O line accumulated in an under-water depositional environment. They are sterile of archaeological remains. We decided, therefore, to stop excavation at this part of Area B and focus in the next seasons on the western squares of lines O – N – M (Fig. 10).

JRD Radiocarbon Dating and Age Modeling

Liz Bunin

A total of 23 charcoal samples from the Jordan River Dureijat excavation have been radiocarbon dated at two laboratories, Beta Analytics in Miami, USA and Poznan Radiocarbon Laboratory at Adam Mickiewicz University in Poland. The reported dates are presented in Table 2 along with their calibrations, done using OxCal version 4.3 (Ramsey, 2009) and the IntCal13 Northern Hemisphere calibration curve (Reimer et al., 2013).

Of the 23 dated samples, fourteen¹ were collected from the east wall of the excavation area at square Q-99, three² come from the south wall at square O-96 and six³ come from cultural layers in the interior of the excavation area. Due to differing layer thicknesses, the absence of internal structure within the individual layers and a lack of marker horizons within the layers themselves, the correlation of dates from the same layer but from different locations in the excavation areas are approximate.

Their relative positions, however, are shown on an idealized stratigraphy presented in Figure 23, where white arrows indicate samples taken from the east wall and brackets indicate the approximate positions of samples taken from other parts of the excavation area. One date, Beta-547491, is not included in the figure as there is more uncertainty regarding its position: This sample may be from the mud underneath layer 5 or may come from a deeper unit, tentatively referred to as layer 6.

We assume that the dated charcoals come from burned terrestrial plant material washed into a low-energy aquatic environment by flowing surface water. The use of terrestrial plants for dating is preferable to aquatic plants or carbonate material due to the unknown reservoir age of the water body, where organisms would take up old carbon in the catchment causing radiocarbon dating to overestimate their ages. There will always be, however, some uncertainty regarding the amount of time that passes between the plants growth, incineration, transportation to the water body and eventual burial.

¹ **East section square Q-99:** Beta-457485, Poz-94159, Beta-547486, Poz-94109, Beta-457487, Beta-457488, Poz-94158, Poz-94107, Beta-54789, Poz-94160, Poz-100258, Poz-100321, Poz-100259 and Poz-100295

² **South Section square O-96:** Beta-457490, Poz-94108 and Beta-547491

³ **Archaeological layers:** Poz-100198 (layer 3A; square O-103), Poz-100197 (layer 3B; square O-101), Poz-100196 (layer 3c; square Q-100), Poz-100320 (layer 4A; square Q-100), Poz-100322 (layer 5; square O-97) and Poz-100323 (layer 5; square O-96)

Because differing plant physiologies affect the isotopic composition of plant tissue in addition to the composition of the available carbon, charcoals submitted to Poznan were inspected and identified by Dr. Dafna Langgut (samples from the east wall and layer 5; marked with an asterisk in Table 2 below) and Dr. Ethel Allué (samples from layers 3 and 4; marked with a dagger in the table below). Even when they were not able to positively identify the plant species, they were able to confirm the suitability of the plant material for dating, ensuring that no roots or aquatic plant materials were submitted, which would be subject to reservoir effects from the water body. Samples submitted to Beta Analytics were not identified, although the laboratory was able to measure in house the $\delta^{13}\text{C}$ of those submitted and this information was used to determine the metabolic pathways of plant material dated; one sample (Beta-457487) was determined to come from a C4 plant and was omitted from age models for the site, although the reported age is very similar to others obtained nearby.

Of the 23 submitted samples, one (Poz-100259) was ultimately too small to measure. Additionally, two samples were measured to be very young. Of these young samples, in the case of Poz-94109, modern carbon at a rate higher than today's indicates that the sample likely comes from a plant that grew after 1950 AD and we suggest that this sample may represent contamination from material above. Beta-547485, determined to be less than 400 years old, is the only sample dated from layer 2 and the sharp and uneven contact between layers two and three is interpreted as an erosional surface that truncates layer 3-0 and the sediments above may be much younger (disconformity) or the young age of this charcoal may reflect disturbance and/or homogenization of sediments in layer 2.

Sediment accumulation in layers 3-5 is interpreted as continuous over the last c. ten thousand years of the Pleistocene (approximately 20 – 10 ka cal BP). The nineteen available AMS ^{14}C dates for this interval shown in Figure 24 will form the foundation of an age-depth model to be created using the modelling software Bacon (Blaauw and Christen, 2011). It is our hope that the model will help to refine the age estimations for the cultural horizons in addition to constraining the timing of environmental change at the site as inferred from the proxy datasets under development.

Table 2: JRD 14C chronology

Location	Context/Layer	Lab. Number	Measured Age [BP]	Calibrated Age, 1σ [BP]	Calibrated Age, 2σ [BP]	Plant Species Identification; Δ ¹³ C [‰]	Subm. Date
East Section	Layer 2 sand	Beta-457485	190 ± 30	-	-	-26.1 [C3]	1.2017
East	Top of 3a	Beta-457486	9570 ± 40	11011 ± 63	10920 ± 182	-25.1 [C3]	1.2017
East	3b	Beta-457487	11270 ± 40	13331 ± 50	13341 ± 95	-11.9 [C4]	1.2017
East	Top of 3b	Beta-457488	11490 ± 40	13331 ± 50	13341 ± 95	-25.3 [C3]	1.2017
East	Bottom of layer 3c mud. Immediately above layer 4	Beta-457489	13320 ± 40	16039 ± 93	16033 ± 183	-24.1 [C3]	1.2017
South	Bottom of 4b stony layer	Beta-457490	14350 ± 40	17541 ± 79	17527 ± 177	-22.5 [C3]	1.2017
South	Layer 5 south wall – not good	Beta-457491	16660 ± 50	200099 ± 93	20103 ± 193	-24.7 [C3]	1.2017
East	Bottom of 3c	Poz-94107	12460 ± 70	14586 ± 238	14625 ± 403	Unidentified*	6.2017
South	Layer 5	Poz-94108	13870 ± 80	16807 ± 157	16781 ± 300	<i>Quercus</i> sp.*	6.2017
East	3a mud (mud below 3a)	Poz-94109	<0 [105.75 ± 0.33 pMC]			Unidentified*	6.2017
East	Middle of 3c	Poz-94158	12350 ± 60	14388 ± 178	14419 ± 321	Probably <i>Olea</i> sp.*	6. 2017
East	3-0	Poz-94159	10010 ± 60	11478 ± 140	11512 ± 242	<i>Q. ithaburensis</i> *	6.2017
East	Below 4a	Poz-94160	13960 ± 80	16941 ± 151	16911 ± 310	<i>Q. ithaburensis</i> *	6.2017
Arch	3c archaeological layer	Poz-100196	12416 ± 47	14491 ± 183	14516 ± 335	<i>Salix</i> sp.†	2.2018
Arch	3b archaeology	Poz-100197	11815 ± 47	13652 ± 64	13675 ± 185	<i>Salix</i> sp.†	2.2018
Arch	3a archaeology	Poz-100198	8887 ± 37	-	10037 ± 149	<i>Juglans</i> or <i>Laurus</i> †	2.2018
East	Top of level 4c	Poz-100258	14433 ± 40	17584 ± 82	17612 ± 188	Unidentified*	2.2018
East	Layer 5	Poz-100259	Too small to date			Unidentified*	2. 2018
East	Mud 10cm above layer 6 (east section)	Poz-100295	16867 ± 71	20352 ± 119	20333 ± 225	Unidentified*	2.2018
Arch	Layer 4 (between levels 4a and 4b)	Poz-100320	13368 ± 53	16091 ± 99	16076 ± 195	<i>Salix</i> sp.†	2. 2018
East	Mud below Layer 5 (east section)	Poz-100321	16612 ± 72	20047 ± 113	20045 ± 240	<i>Salix</i> sp. or <i>Populus euphratica</i> *	2.2018
Arch	Archaeological layer 5	Poz-100322	14414 ± 58	17566 ± 95	17582 ± 222	<i>Salix</i> sp. or <i>Populus euphratica</i> *	2.2018
Arch	Archaeological Layer 5	Poz-100323	16549 ± 72	19972 ± 117	19948 ± 242	<i>Salix</i> sp. or <i>Populus euphratica</i> *	2.2018

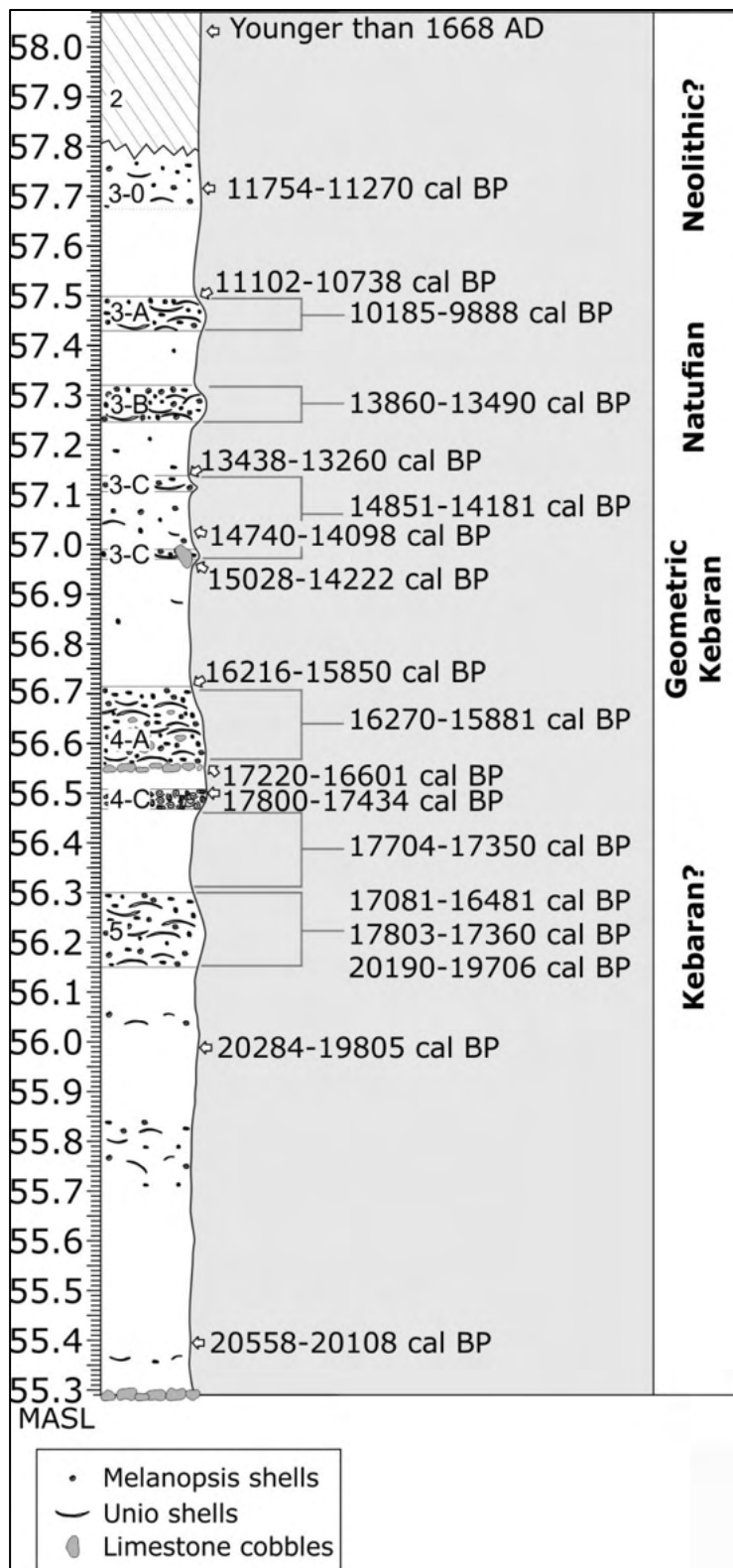


Figure 23: Ages of dated charcoal samples to be included in future age models. Calibrated dates were produced using OxCal version 4.3 and are shown as calibrated years before present (BP). Ages are reported as 2-sigma ranges except in the case of Layer 2, where the age shown reflects the maximum age within two-sigma uncertainty as determined by OxCal. Brackets indicated the approximate stratigraphic levels for samples recovered from the excavation area and south wall. Layer 4-B is shown as a pavement of cobbles centered at 56.55 MASL

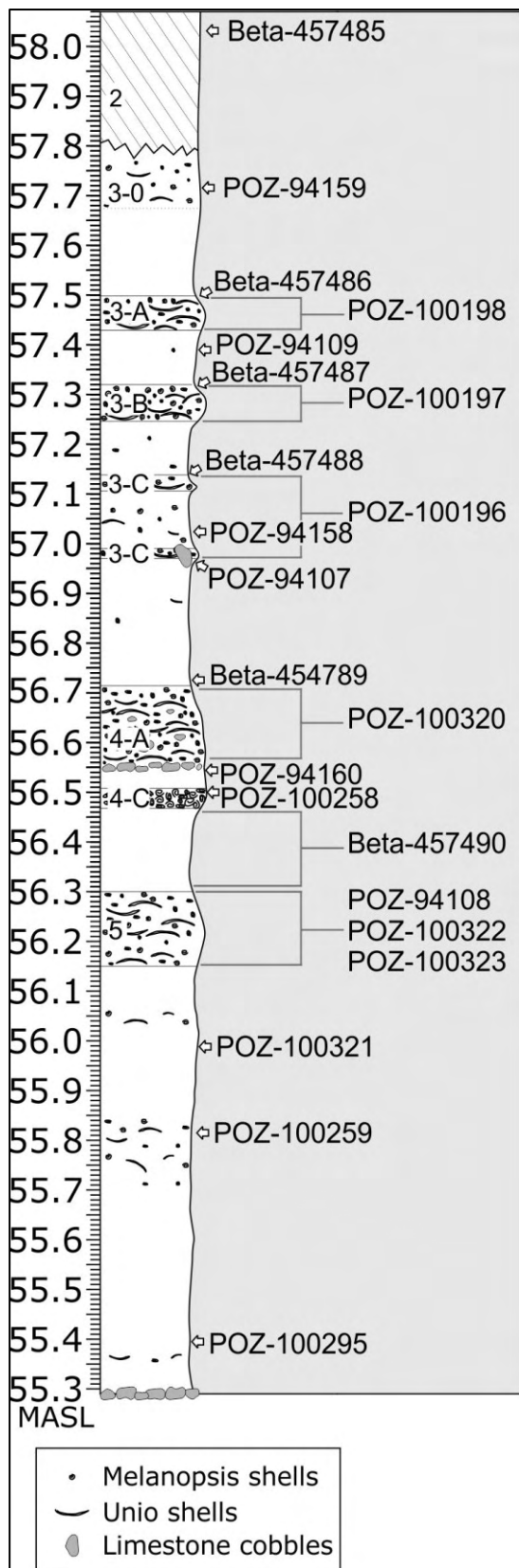


Figure 24: Lab numbers for dated charcoal samples. Brackets indicate the approximate stratigraphic levels for samples recovered from the excavation area and south wall relative to the east wall stratigraphy. Layer 4-B is shown as a pavement of cobbles centered at 56.55 MASL.

JRD 2017 EXCAVATION SEASON

The 2017 excavation season at JRD took place between August 21 and September 14, 2017; Excavation permit – G-89/2017, renewal of permit G-68/2016. The team included some 40 students from the Tel-Hai College archaeological excavation field school (each participating in 2 weeks of excavation) and volunteers from Iceland, Sweden, Czech Republic, UK, USA and Israel. Area supervision, recording, and measuring were conducted by Francesco Valletta and Laura Centi (Italy, The Hebrew University).

The primary objectives of the 2017 excavation season were:

1. To continue excavating the site layers exposed during the 2016 season.
2. To expose Layer 5, only exposed at a small area in previous seasons.
3. To focus excavation of the upper, Natufian layers of the site, Layer 3a and 3b, primarily exposed at the northern part of Area B (see below).
4. To further refine the chronology of the site layers by collecting controlled samples for ¹⁴C dating.
5. To extend the geo-archaeological sequence of the site by deepening the type section (Section East – see below).
6. To dig a deep test pit into the deep layers of the site (below Layer 5) in order to explore the lower sequence of the site.

Excavation methodology

Area B was marked by a 1-square meter grid, part of the general grid projected on the entire site. Each square was subdivided into four 50²cm sub-squares (Fig. 2). Each excavator was in charge of 1-square meter. The excavation was recorded by each of the excavators on a daily page (See Appendix 1). The excavation was executed using 5 cm spits and all finds (>3cm) were left in place and recorded in situ prior to removal from the square. Recording of the artifacts was done by Leica Total Station device. Smaller finds were collected into “general bags” sorted by material (flint, bone, botanic etc.). All soil samples and other important features were also recorded by the total station. All sediments were collected in buckets and sieved in the Jordan River using 0.2mm mesh sieves. In some cases, for example in layers sterile of finds, only a sample of sediments was collected. In most of these cases, sampling was of a single bucket per spit per square. Any sampling of sediments was noted in the daily

excavation page. All daily pages are part of this report. Sediments and pollen samples were collected by the geology (S. Mischke and L. Bunin) and pollen (D. Langgot) experts using their own specific methodology. All samples were recorded by the total station for location data.

Between seasons, the excavated area is covered by sediments for protection and preservation. Hence, at the beginning of each season the site is measured to ensure the accuracy of the reopening and attachment to the previous year's grid. At the next stage, the sediments are dug using a JCB excavator to expose the excavated surface. The final pre-excavation cleaning of the last 10-20 cm of sediments is done by hand to prevent damage to the excavated surface.

Area B Northern Squares - Layer 3a & 3b Natufian

The results of the 2015 excavation season indicated the presence of archaeological layers at the top of the sequence that were not excavated due to their exposure by the tractor shovel during the opening of Area B at the beginning of the 2015 season. These layers, identified immediately under the sandy Layer 2, were visible at the northern section of Area B and were lying below the exposed surface of the 2014 test excavation of Area B1. Eight additional squares were opened in 2016 to the north of Area B, limited to the north by the 2014 Trench 2 (Fig.10). During the 2017 season, excavation at these squares continued and an additional two squares were open toward the east of this part – squares R-102 and R-103. See the JRD 2016 IAA report for description of the early stages of excavation at these squares prior to the 2017 season.

Upper Natufian Layers - Layer 3a

The layer was exposed at the north squares of Area B, in lines 102-103 (Fig. XX). The work here continued from the point reached at the end of the 2016 season. During the 2017 season, an additional two squares were opened and excavated toward the east: squares R102 and R103. Excavation here was careful and slow, with the wealth of finds making excavation even slower. Layer 3a here was subdivided roughly into stages – primarily 3ai and 3aii. This separation is not clear-cut in all squares and the stratigraphy changes on an east to west line. Nevertheless, at some of the squares these horizons are real and visible.

The richness of the archaeological finds, primarily in the 3aii horizons, dictates the establishment of a specific finds recording and collecting method. All artifacts and finds are left un-removed by excavation. Recording includes photography and map drawing. On the map (Fig. XX) all flint and bones (>2-3 cm) are drawn. Large and notable limestones (un-fragmented, >3cm) and basalt (>5cm) are also drawn. All artifacts are recorded using a total station device. Artifact total number is, in most cases, noted on the map as well. Collecting and keeping of finds is managed as follows:

- Most of the lithics of the layer are small (>5cm) basalt pebbles. These pebbles are noted on the map as raster, counted per square and not kept.
- Basalt > 5cm are all recorded by total station. Artifacts (flaked pieces, flakes, hammer-stones, net-sinkers) are collected and kept. Other, non-artifact larger basalts were not kept.
- Limestone > 5cm are all recorded and kept.
- Limestone < 5cm are collected in general bags per spit per sub-square. The level for each general bag is recorded for the entire spit.
- Flint and bones – all finds > 2cm are drawn on the map and collected.
- One sub-square was selected for sampling. In this sub-square all artifacts, including all basalts and limestones were collected.
- Botanical remains are rare in these layers, possibly due to drying of the sediments during recent years. Sizable pieces of wood and charcoal were, of course, collected and recorded.

Layer 3a stratigraphy and interpretation

The exposed surface of layer 3a and its sub-levels as observed at the end of the 2016 season is presented in figures 26 and 27. Excavation during 2017 continued exposing these layers and clarified some earlier observations and assumptions. It seems, currently, that the stratigraphy and context of layer 3a is best understood when the area is described horizontally, as the nature of the sediments and human occupation change between squares at the same level. The chronology represented within the Layer 3a levels is unsettled. The question is whether the different levels represent different occupation stages over a considerable time period or whether they are simply different uses of the surface for different activities. Two charcoal samples were sent for 14C dating which may contribute to our understanding of the issue (see Table 2).



Figure 25: Layer 3a and sub-stratigraphy at the end of the 2016 season



Figure 26: Layer 3a ii at level 57:25

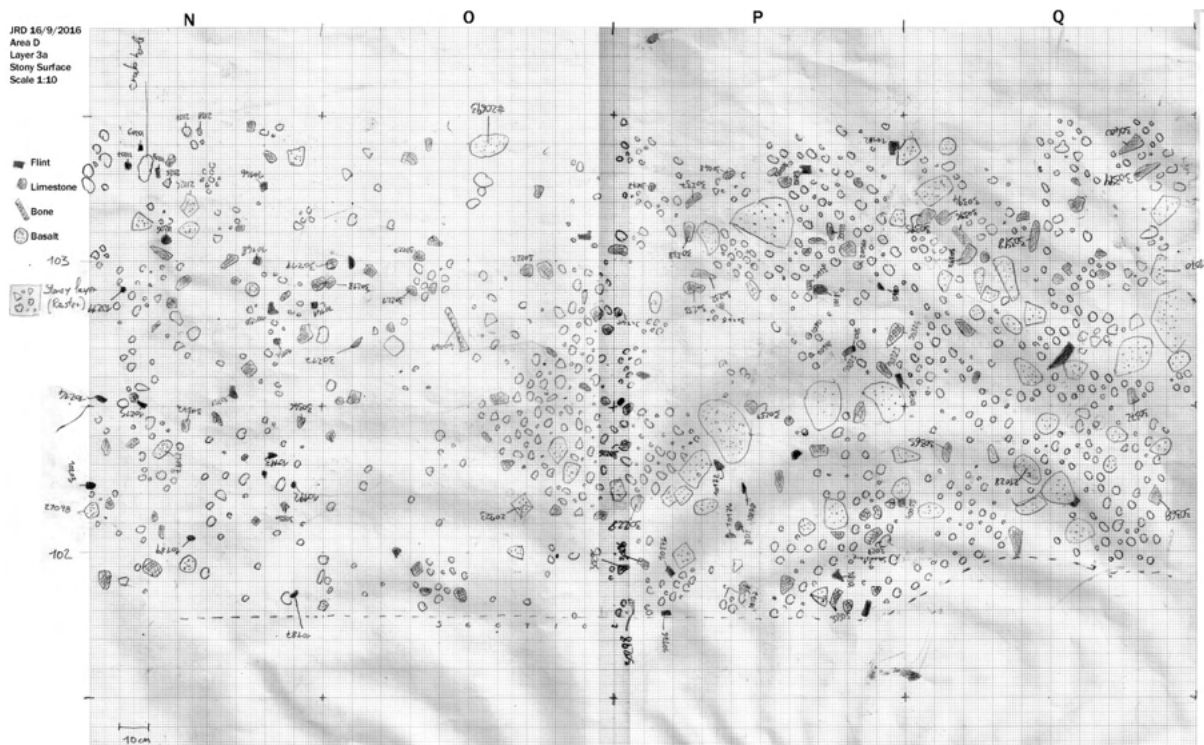


Figure 27: Layer 3a at the end of the 2016 season

The context of layer 3a at the end of the 2017 season is understood as changing horizontally along the exposure. It seems that the exposed surface can be subdivided into three different units representing different accumulation contexts.

As can be seen from Figures 27-29, the western part of the exposed area, starting at the western half of the P squares and spreading westward, is characterized by the presence of larger basalt stones, up to 30 cm in maximal length. This type of surface was also exposed in the R squared excavated in this area during the 2017 season (Figs. 30-31). When observing the large basalt stones exposed, it seems that their arrangement is not random. In addition, it should be noted that the sediment between the stones does not indicate a high energy accumulation environment (e.g. stream). It is suggested that all of the stones in the layers were brought by the site's inhabitants and possibly placed in order. Determining that the order represents walls seems a bit exaggerated but some arrangement can be observed. In addition, difference in artifact density was noted between different parts of the surface, such as north and south of the stone line. This observation will have to be tested statistically before discussed further.

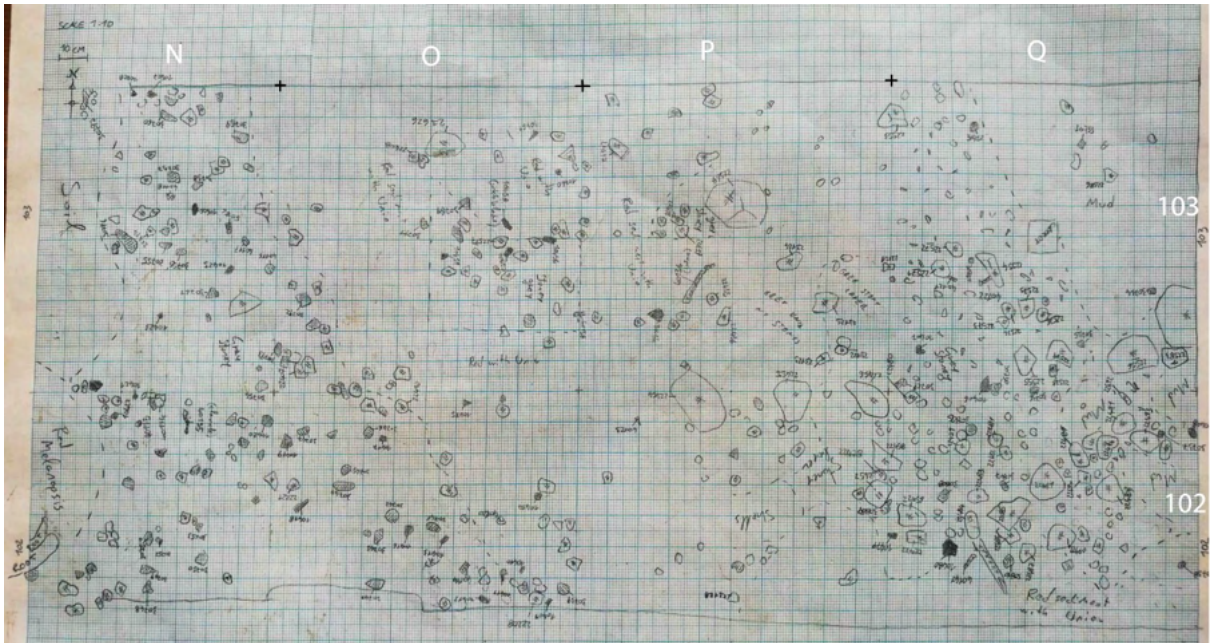


Figure 28: Map of Layer 3a 2017

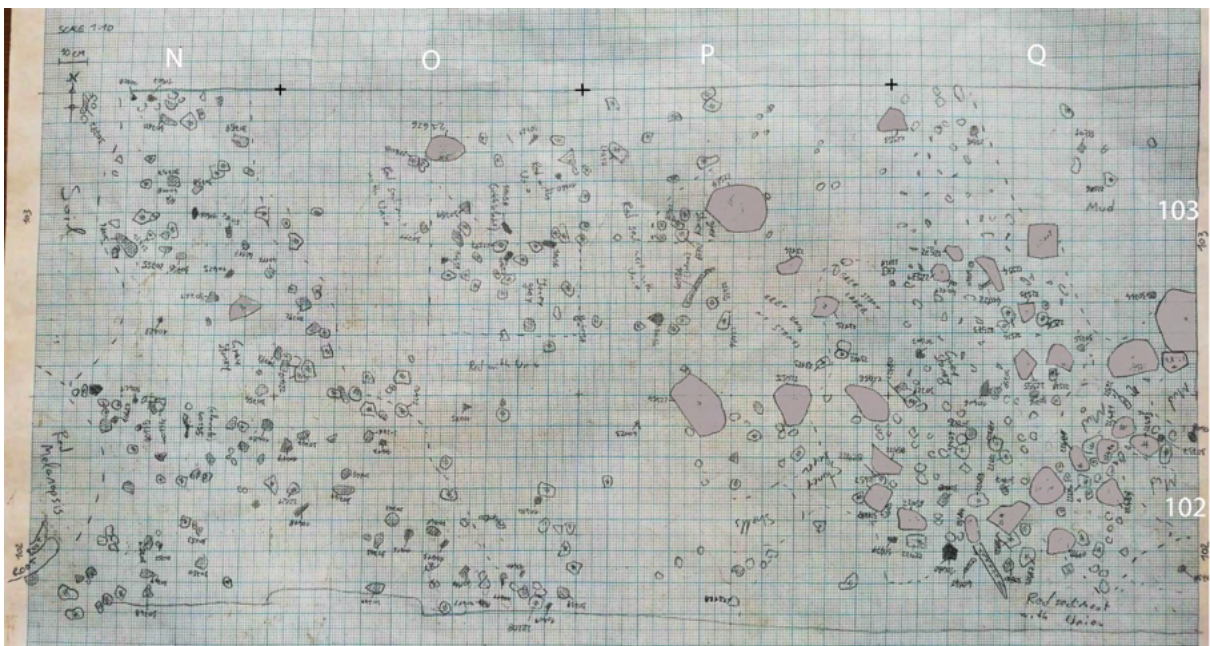


Figure 29: Map of Layer 3a 2017 with large basalts emphasized

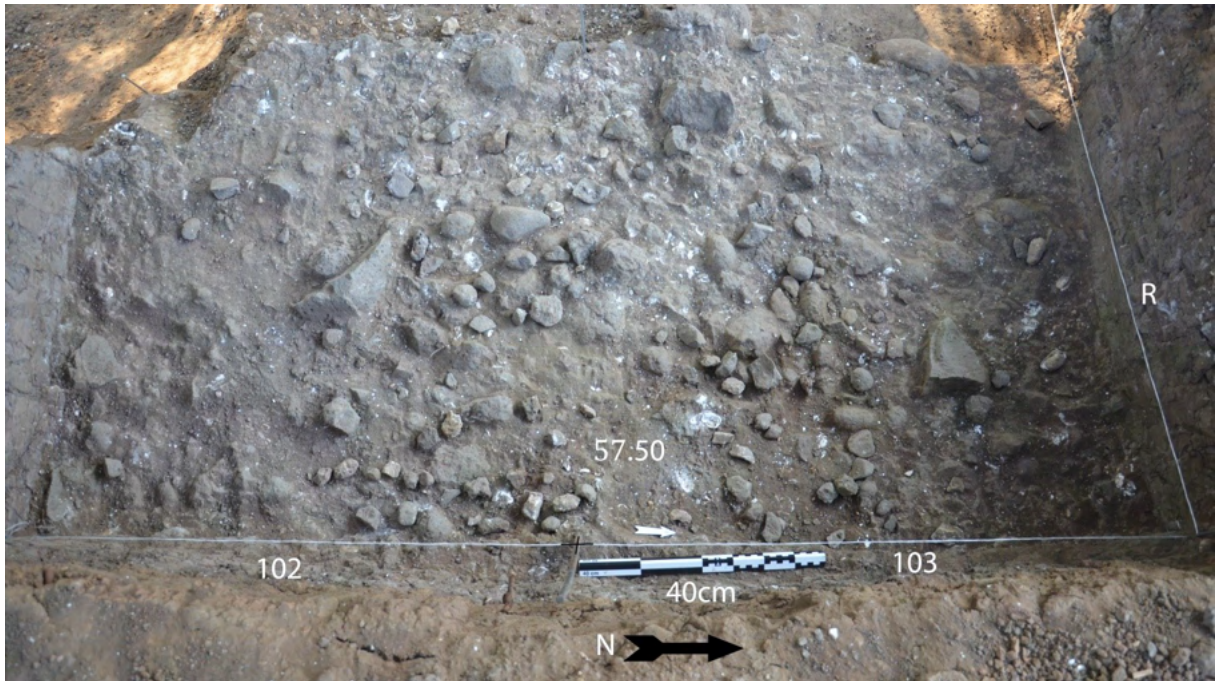


Figure 31: Layer 3a in squares R-102 and R-103

A possible explanation for the high density of large basalt stones may come from the presence of a shallow pit, dug into the sandy layer below layer 3a here, exposed during the 2017 season. The pit, marked as Locus 10, filled by shells, flint, and small basalt cobbles is also visible in the square Q-102 south section (Fig. 32-33, 36). The primary find in the context of the pit are human remains, including a broken tibia, a rib fragment, and two teeth (figs. 34-35). It is suggested that the pit represents a shallow burial that was later disturbed. The presence of additional human bones scattered on the 3a_{ii} surface to the west (Fig 37) supports this suggestion. It should be noted that the human bones found during the 2015 season at square N-100 & N-101 (a mandible and a tibia; see 2015 IAA excavation report) may have belonged to the same individual and were found in a similar level. The 2015 bones were found within the “red Melanopsis” sandy horizon to the west of layer 3a – see below.



Figure 32: Locus 10 in Section 101 north



Figure 33: Locus 10 during excavation



Figure 34: human bone at layer 3a square Q102



Figure 35: Human bone at square Q102c Layer 3a

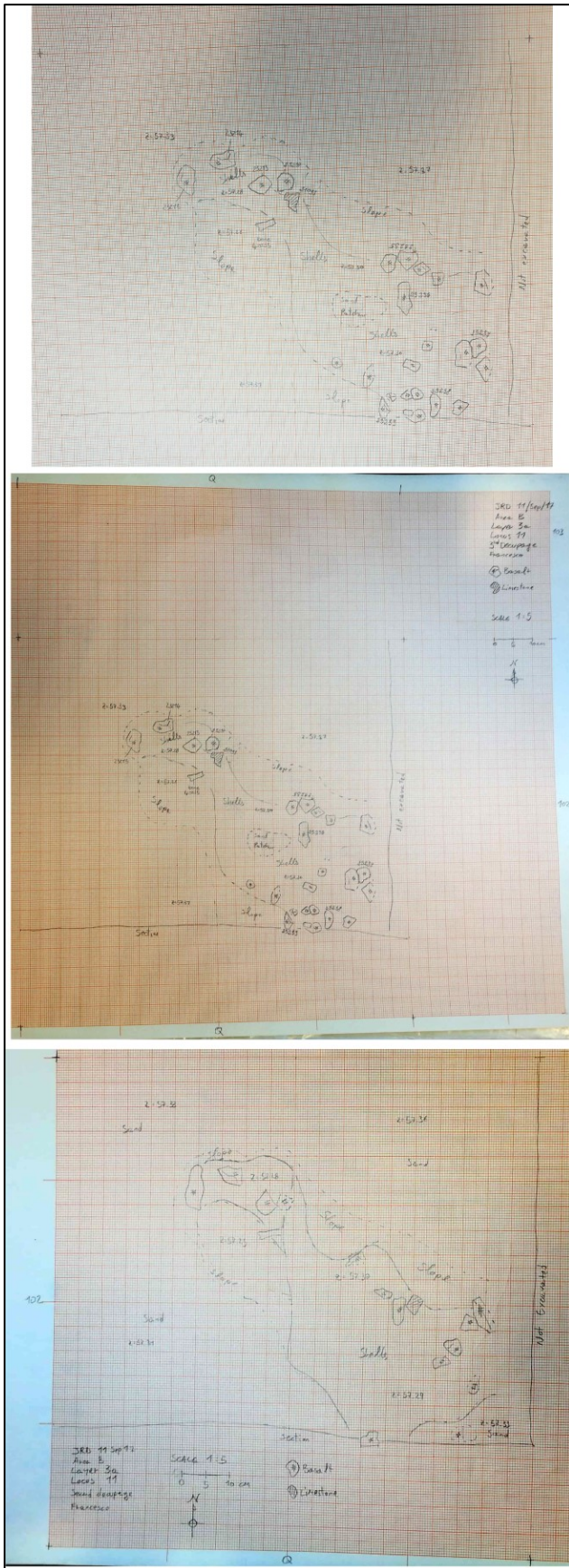


Figure 36: map of 3 stages of Locus 10 Square Q102

The “center” part of the exposed 3a surface, from the middle of the P square and westward toward the N square, is of a different nature. Layer 3a levels here, Level 3ai and 3aii, are of a similar nature – they are comprised of a high density of *Unio* shells, most of them as separated valves but, in some rare cases, complete, both valve specimens are observed. The sediment is sandy in nature and contains numerous small basalt pebbles, flint artifacts and bones (Figs. 26). Basalt cobbles larger than 5 cm in size are rare. It seems that no spatial pattern can be seen in this level. It is suggested, hence, that the nature of the layer is of a garbage dump – a midden. The main component of the garbage was the *Unio* shells. This may suggest that the shells were collected and consumed in large numbers. This hypothesis must be further studied and supported before confirmed.

Among the finds in this layer are sporadic botanical remains (except for charcoal which is found in large numbers). In Square P103 a large branch was found, in completely dry conditions (Fig. 38).



Figure 37: Human bone layer 3a



Figure 38: Wood remains (dry). Layer 3a Square

At the western edge of the 3a surface a disturbance from the west can be identified. A layer, primarily comprised of *Melanopsis* shells in sandy matrix has a sharp and clear contact with the 3a layer (Figs. 40-41). The layer is reddish in color, probably due to oxidation, that may have resulted from the short distance to the water of the Jordan River. Archaeological finds are much less frequent in this layer. It may be a layer of younger age penetrating from the west and eroding the Layer 3a matrix or, alternatively, this layer may represent changing water level in the water body at the time of occupation, possibly at closer proximity to the lake's shoreline, which resulted in a different nature of sediments. In either case, the "red *Melanopsis*" marks the western end of the 3a levels.

The contact between Layers 3a and 3b in these squares is becoming less clear. In the eastern part of Area B, Layer 3a and 3b are separated from one another by a layer of mud. In the north, this mud layer is getting thinner and eventually it seems that the two layers merge together in squares line 101 or 102 (Fig. 39). This stratigraphic question will be further explored in the next seasons.

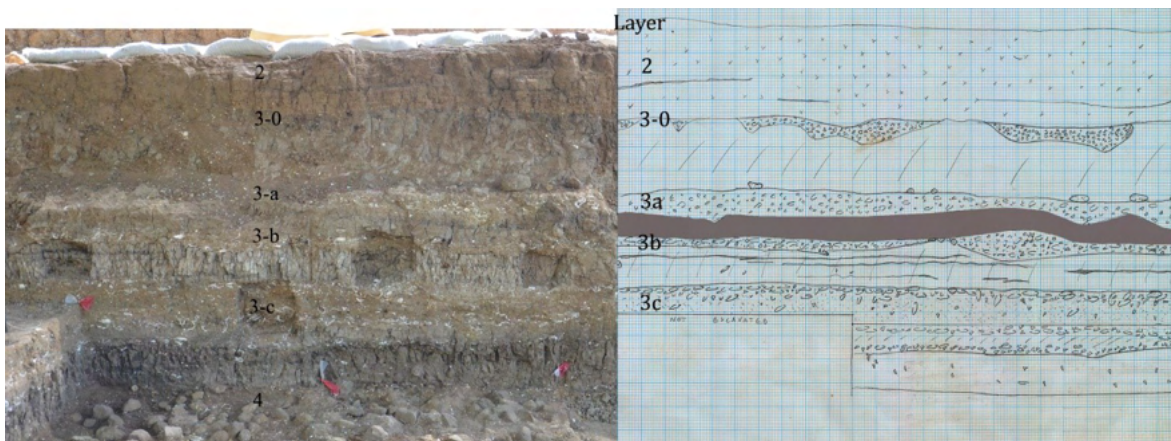


Figure 39: Clear mud layer separating Layers 3a and 3b in east section of Area B

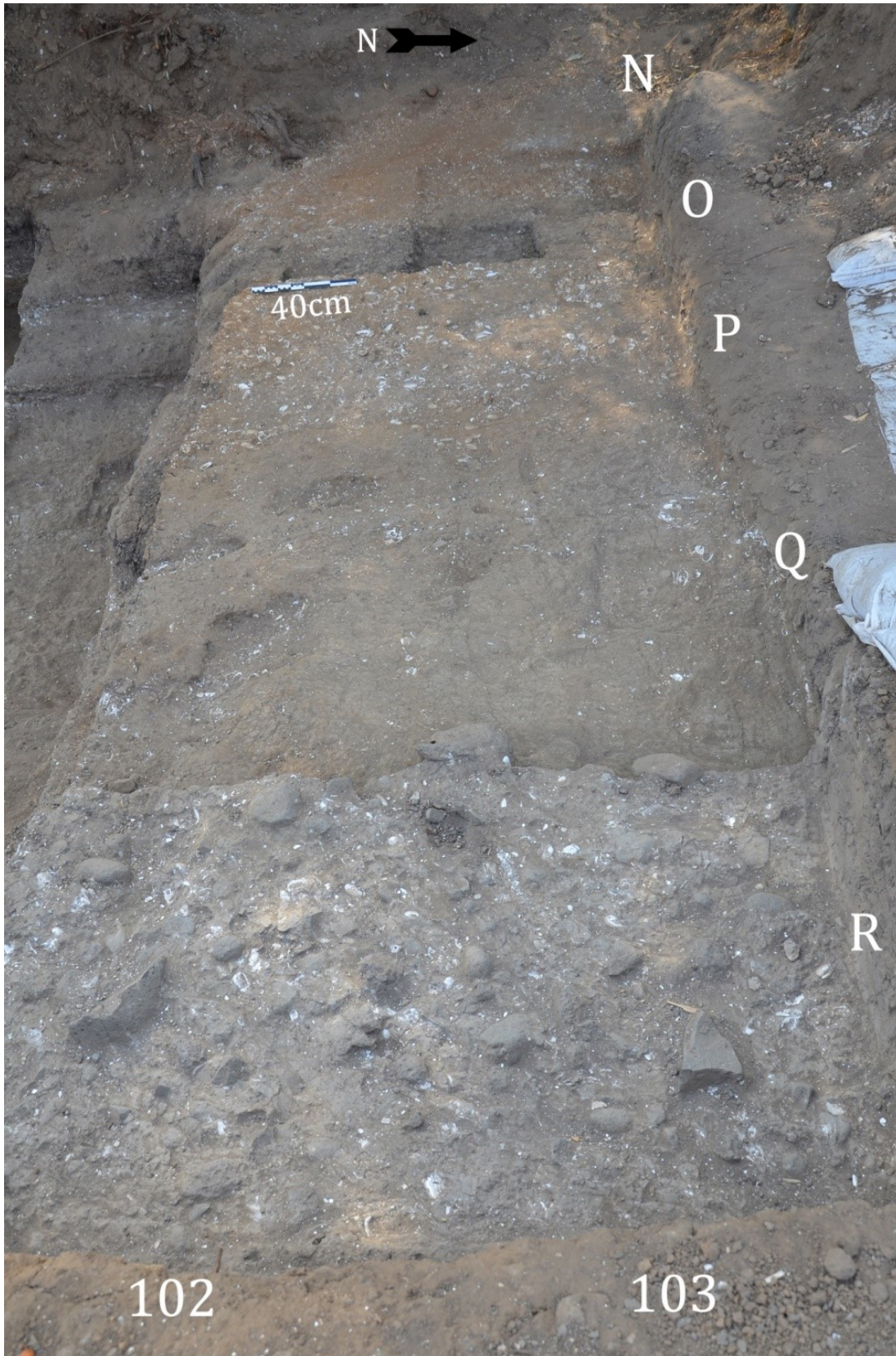


Figure 40: Excavation of Natufian Upper Layers 3a 7 3b at the end of 2017 season

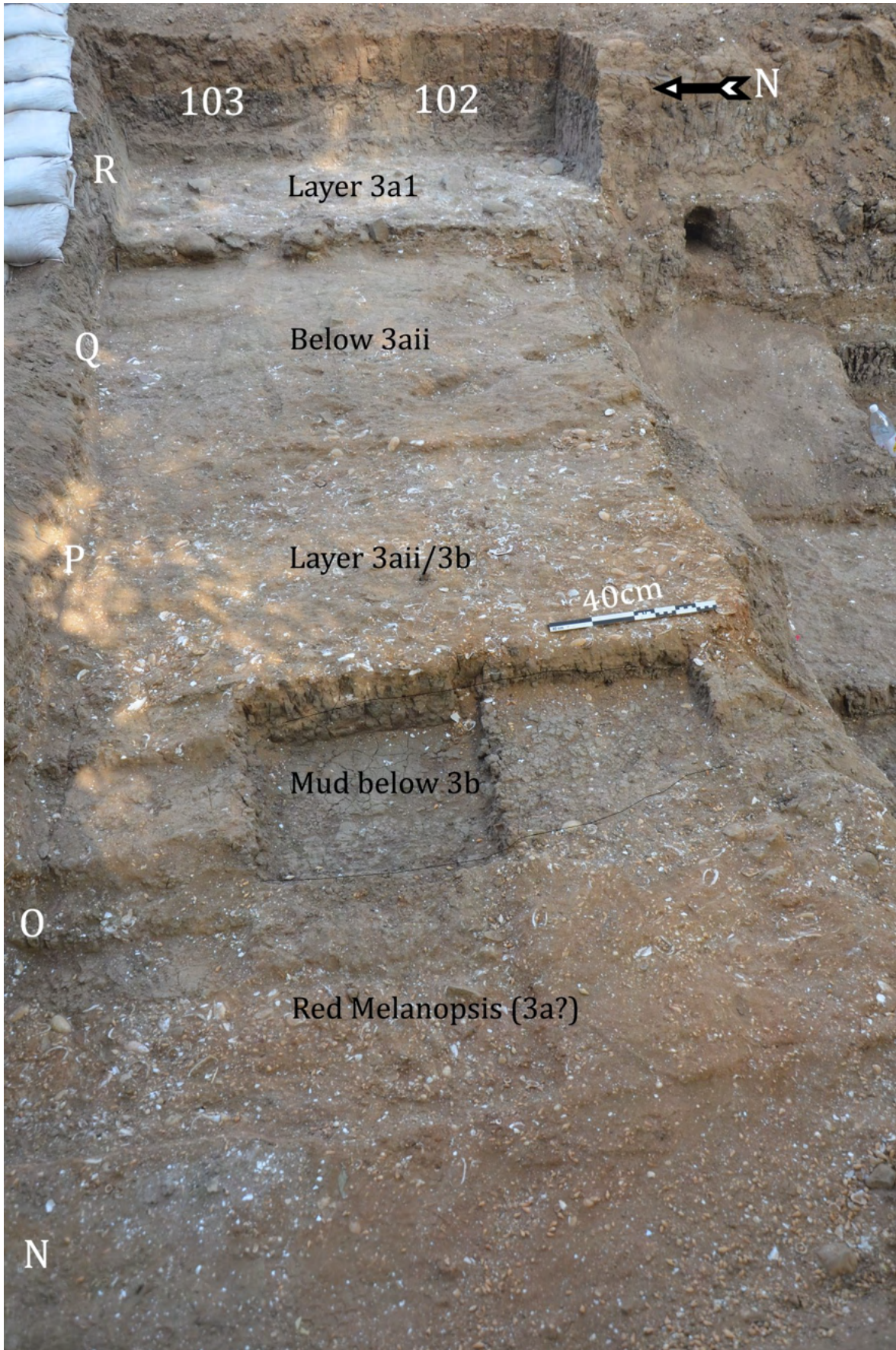


Figure 41: Stratigraphy at the end of 2017 season

Layer 3c

Layer 3c was excavated only in square O-101 in the beginning of the season at square P-101, primarily in an attempt to remove the final remnants of this layer before reaching layer 4. Layer 3c not only is getting thicker toward the west but also seems to decline down toward the west, possibly into the margin of Layer 4 in the M squares and creating the stratigraphically mixed context squares in the west M line in these layers. Only in 2017, we observed that under this mixed layer 4, a thick layer of mud was deposited under which Layer 5 is well defined (Fig. 12).

Layer 4

At the end of the 2016 season, we assumed that Layer 4 was removed in most squares of Area B. This layer, typically a “pavement” of basalt cobbles, limestone net sinkers with a low frequency of bones and flint tools, was named Layer 4b horizon. Above it are the 4a layers characterized by alternating and sometime mixing horizons of mini-shell and *Melanopsis* shells named Level 4a. Below the stony horizon of Level 4b was a thin layer of mud (less than 5 cm in most places) and below it a thin horizon of lake shore material, only a few cm in thickness, defined as Level 4c (also known as the François layer; Fig. 11). This stratigraphy did not change during the 2017 season, yet the nature of the Layer 4 levels and their spatial distribution becomes more complex.

Excavation at the easternmost squares of Area B (square line Q), where a horizon of stone cobbles was already removed during the 2016 season, exposed an additional horizon of basalt cobbles and limestone net sinkers (Figs. 42-43). It seems that the 4b horizon is thicker than expected and, possibly, in the eastern squares of Area B, may actually comprise two separated horizons of cobbles. All stones larger than 5 cm in the layer were recorded, allowing us to test the nature of the level and the horizontal distribution of the finds using GIS in the future.

An additional Layer 4 stratigraphic issue arose from the excavation of the stony horizon of Level 4b in the square in the center of Area B, the O squares. Here, it seems that the 4b horizon of basalt cobbles and limestone net sinkers is covering the entire surface, with no observable change in the nature or size of the stones, but the matrix to which this horizon is

deposited changes from dark mud to a shell-rich (unioid), lake-shore sediment. This is a clear change in the nature of the sediment that the archaeological horizon seems to “ignore” (Figs. XX). The explanation suggested for this observation is that the archaeological horizon of Level 4b was formed by the site’s inhabitants on the shore of the paleo-lake. The shore is not a uniform, unchanged horizon but is formed of mud to the east and beach material to the west (suggesting that the water body was, at the time, located to the east of the site). The Level 4b fishermen left their artifacts and stones regardless of the sedimentology. This observation further supports the assumption that the stones of Level 4b were all imported to this locality by human activity.

The Level 4b artifacts excavated in 2017 are similar in nature to the upper part of this layer excavated in 2016. At the northern squares of O-101 & N-101, broken basalt cobble-sized artifacts were found that may come from a large broken grinding stone. This is additional evidence for the recycling of basalt grinding elements, probably as net sinkers, as observed for the broken pestles found previously in this layer.



Figure 42: Layer 4b (lower part) at squares Q-98 Q-99.



Figure 43: Layer 4b Lower in squares Q98 & Q99

Below Layer 4

The results of the 2017 excavation season enabled us to suggest a reconstruction of the complex stratigraphy observed below the stony horizon of Level 4b. The primary observation is that a line of unconformity is observed all along Area B, separating the area into two parts along the north-south axis. This line, crossing Area B along the eastern part of square line O (Fig. 44) is observed all along the sequence, but below Layer 4 it displays an intense shift in sedimentation, probably reflecting a very different accumulation environment. It seems that the sediments below Level 4b east of this line were accumulating in an underwater environment that deposited mud with changing amounts of *Unio* shells. No human activity is observed at this part of area B. Level 4c is either absent here or merged into the lower part of Level 4b, and Layer 5 is only (possibly) present in the form of a rich shell horizon within the mud (Fig. 22).

The picture to the west of this line is completely different. The Level 4b stone horizon is disturbed in the west square lines of the N squares and even more so in the M square line (Fig. 44). Layer 3c is slanting down and merging with Layer 4, sediments from the west are wedged into layer 4 here creating a hard to interpret sequence. Below Level 4b the picture becomes clearer. A clear, thin (c. 5cm) mud horizon separates Level 4c from the upper layers.

Below this level is additional, thick mud (getting thicker toward the west, reaching more than 20 cm in thickness) which overlies Layer 5 (see description of Layer 5 below). The rich archaeological Layer 5 at the west half of Area C seems to have been deposited into a depression in the sediments, possibly an old channel or a shoreline.



Figure 44: Section south of Area B end of 2017 season. Stratigraphic difference between east and west parts of Area B below Layer 4.

Few explanations can be suggested for the cause of the dramatic shift in sedimentation between the two parts of Area B. First, it seems that at least during the lower stages of the stratigraphy, the water body was located toward the east and the shoreline was to the west. The clear-cut distinction between the two parts of the site may be explained as resulting from tectonic activity, as suggested by the observation at the deep sounding of O-96 (see above). The water eruption that pushed Layer 6 into upright position supports the occurrence of some post-depositional tectonic activity involved in the forming of the stratigraphy here. This can also explain the accumulation of shoreline deposits of Layer 5 to the west in what is today a lower location than the lacustrine sediments of Layer 5 to the east.

Layer 5

Layer 5 was exposed at the end of the 2017 season in a relatively small surface of Squares O-96 and O-97 and in the N line Squares N-96 to N-99 (Fig.10). The upper part of this layer was also reached in Square M-99. Layer 5 is rich in archaeological finds including numerous flint tools, bones, botanical remains (including, for the first time at JRD, large well-preserved wood pieces) and limestone. Stratigraphically, it seems that the layer gets thicker toward the west but the exact thickness has not yet been exposed. Currently, it seems as if the layer was deposited into a depression in the sediments or into an old channel-like low section (Fig. 44). It may also be a shoreline topography that was moved by tectonics. One of the aims of the 2018 season is to continue excavation and analysis to understand the nature of accumulation in this layer.

The nature of the layer deposits is presented in Figs 45-49. As mentioned above, it is rich in finds and includes well-preserved botanic remains. In square N-98c a limestone nummulite fossil was unearthed in the archaeological horizon (Fig. 45).



Figure 45: Layer 5 surface at square N-98c



Figure 46: Layer 5 surface. Square N-96d



Figure 47: Layer 5 surface lower. Square N-96



Figure 48: Layer 5 surface. Square N-97



Figure 49: Layer 5 surface. Square N-98

An additional character of Layer 5 is its wet sediments. Because of its depth, this is actually the first layer at JRD that remained wet and waterlogged since its accumulation and was not subjected to drying in the years since drainage works in 1999. The outcome is the presence, for the first time in JRD, of large pieces of wood in wet conditions. The largest wood piece was excavated in Square M-99 (Figs. 50-53).



Figure 50: Wood in Layer 5 Square M-99



Figure 51: Wood in and charcoal Layer 5 Square M-99



Figure 52: Layer 5 at square M-99 Level 55.57



Figure 53: Removal of wood in Layer 5 Square M-99.

JRD Fauna

Natalie D. Munro

Analysis of the JRD faunal assemblage recovered during the 2015, 2016, 2017 excavation seasons was recently begun. The fauna includes large bone fragments >1 cm that were hand-collected during excavation and smaller faunal material that was carefully picked from dry-sieved sediments that was unable to pass through the 2 mm screen (usually <1 cm).

The fauna has been sorted by excavation season and archaeological layer, and analysis is proceeding layer by layer through each season of material beginning with 2015. Data analysis begins by sorting the identifiable fauna from the unidentifiable bone fragments. Next, data is recorded from each identifiable bone when available and entered into an Excel database. Data categories include taxon, element, bone portion, side of the body, age, sex, gross length and other more specific measurements. A number of taphonomic variables are also recorded including burning, breakage, root etching, weathering, cutmarks, carnivore and rodent damage. The analysis will focus both on (a) taphonomic analysis to determine the primary collector of the fauna (i.e. human, carnivore or natural collectors such as fluvial action and natural death) and (b) taxonomic analysis to reconstruct environments and determine which animals were hunted and collected by humans for dietary purposes.

A small pilot study of bones from the large faunal fraction recovered from multiple contexts revealed an extraordinarily diverse vertebrate fauna. In a sample of only 60 identifiable bones, multiple species of mammals, birds, reptiles and fish were identified. Mammalian taxa are most common and are represented by small game such as hare (*Lepus capensis*), carnivores like wolves (*Canis lupus*), and a number of ungulates including red deer (*Cervus elaphus*), fallow deer (*Dama mesopotamica*), mountain gazelle (*Gazella gazella*) and wild boar (*Sus scrofa*). Initial sorting of the fauna recovered from the picked sediments revealed that fish, snakes and rodents are the most common taxa in the small fraction. The presence of a range of both terrestrial and aquatic taxa (fish, waterfowl and freshwater turtle) suggest that humans chose this lakeside setting for its ecotonal properties, which enabled broad spectrum foraging.

Site preservation and closing

At the end of the season, a map showing the elevations reached in each and every square was recorded (Fig. 54). In accordance with the conservation program of the site, the exposed layers were covered by thick plastic sheet (Fig 55) to mark the excavated surface. The entire excavation area was then covered by sediments (Fig. 56). This is done to protect the layers from exposure to atmospheric conditions during the year, to prevent weathering of the sediments due to winter water flooding and also for safety reasons. The site was left totally covered by soil (Fig. 57). In recent visits to the site during the 2018 winter (which was, unfortunately, mild), it seems that the site covering is holding well.

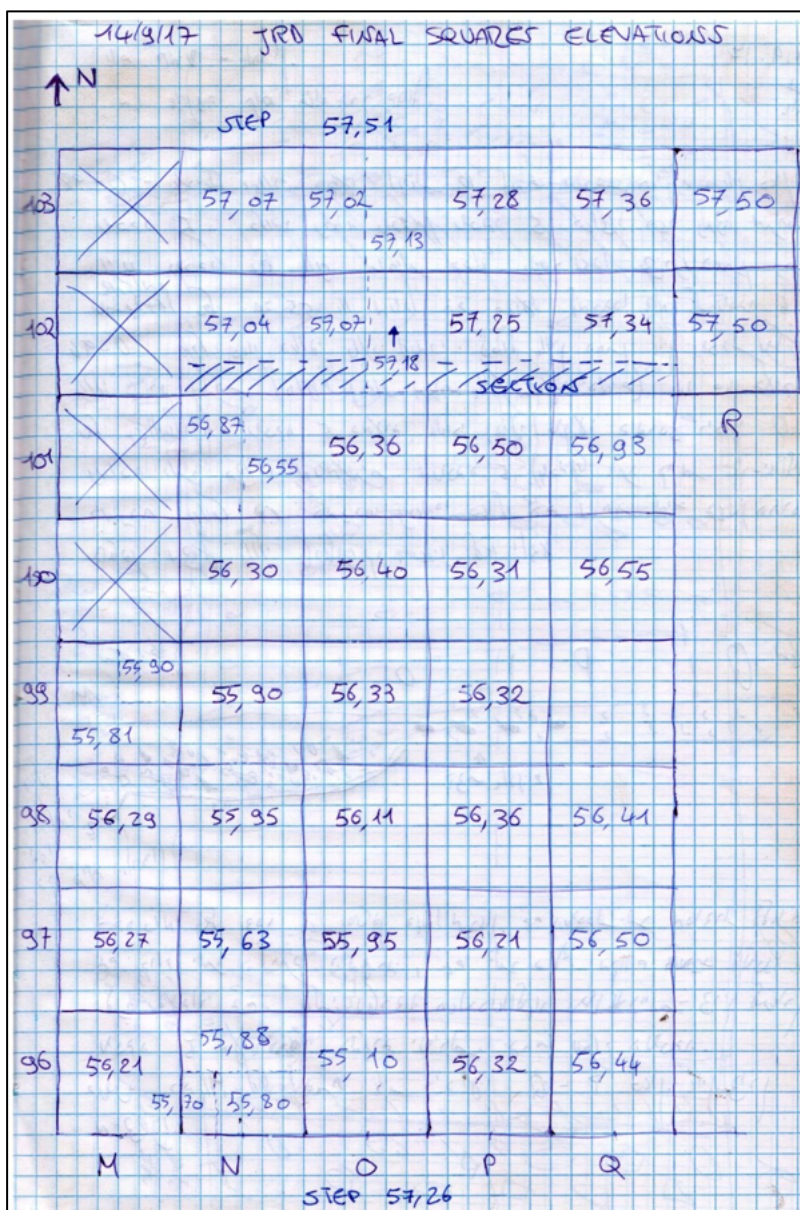


Figure 54: Final elevation map of Area B at the end of the 2017 season (from the field notebook)



Figure 55: JRD Area B covered before closing



Figure 56: Covering Area B at the end of the 2017 season



Figure 57: JRD at the end of the 2017 season

Directions for future excavations

The goals of the 2018 season are:

1. To open a significant surface of the Natufian layers at the northern part of Area B (see map).
2. To excavate Layer 5 at the western section of Area B.
3. To open a test small excavation area north of Area B.
4. To collect samples for refined chronology and for the different research collaborations (flora, fauna, geology and more)

The 2018 excavation plan:

We will continue excavating in Area B.

Excavation at the northern sector of Area B will focus on the exposure of the Natufian Layers at the upper part of the site's stratigraphic sequence (Fig. 1). We intend to open an additional 6 to 8 squares here to expand the surface excavated of the Natufian.

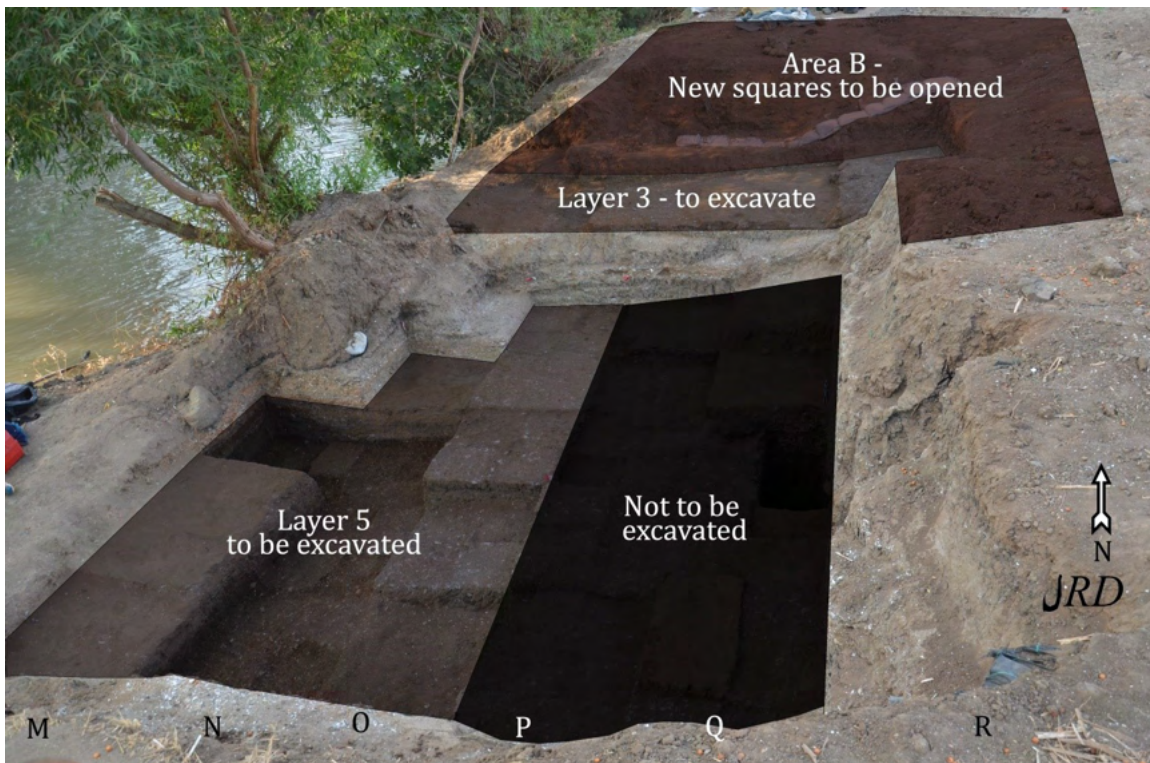


Figure 58: JRD 2018 work plan

At the southern (main) part of Area B, during the 2017 season, layer 4 was completely removed from the entire area. The results indicate that at the eastern part of Area B, Square lines P and Q (see Fig. 1) Layer 5 accumulated under water and show no evidence for human activity. These squares are not to be excavated during the 2018 season. On the other hand, toward the west (squares lines M-O), Layer 5 is thick and rich with finds. During the 2018 season, the squares to the west of Area B will be excavated with the goal of exploring this rich and interesting layer.

Conclusion and significance

The Levantine Epipaleolithic (EP; 23,000 to 11,500 years ago) was a period of unprecedented socioeconomic change beginning at the Last Glacial Maximum with nomadic bands of hunter-gatherers and ending with Natufian sedentary communities. The excavation at Jordan River Dureijat (JRD) unearthed a well-defined stratigraphic sequences. JRD is unusual for its outstanding preservation of organic remains, which will enable establishment of a high resolution chronology for the entire Levantine EP. The archaeological horizons of JRD document >10,000 years of repeat visits by hunter-gatherers to a preferred spot. The unique lithic assemblage comprises well-defined typo-chronological markers (microliths) but the

primary finds are fishing equipment and numerous fish bones. JRD, is, therefore, a logistic hunting (fishing) station located at the outskirts of the large EP sites of the Hula Valley such as Eynan (less than 10 km to the northwest). This unique, task-specific, short-term sequence of occupations will enable us to explore changing mobility patterns and modes of subsistence during the EP.

The JRD layers contain uniquely well-preserved paleoenvironmental proxies including rich macro- and micro-faunal assemblages, ostracods, seeds, fruit, wood and charcoal, well-preserved pollen, and an exceptionally rich mollusc assemblage. These proxies will enable the development of models explaining the impact of climatic and environmental changes between the LGM and the Holocene interglacial and their interrelationship with fundamental changes in human ways of life, from hunter-gatherer groups to sedentism and the establishment of agricultural communities of the Neolithic.

References

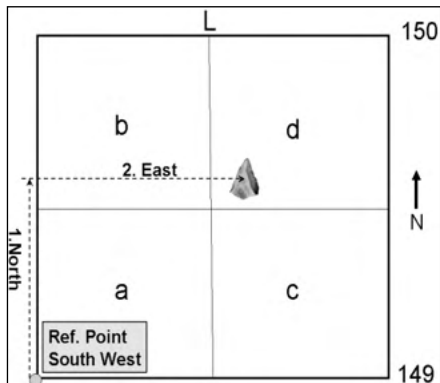
- Blaauw, M., Christen, J.A., 2011. Flexible paleoclimate age-depth models using an autoregressive gamma process. *Bayesian analysis* 6, 457-474.
- Marder, O., Biton, R., Boaretto, E., Feibel, C.S., Melamed, Y., Mienis, H.K., Rabinovich, R., Zohar, I., Sharon, G., 2015. Jordan River Dureijat - A new Epipaleolithic site in the Upper Jordan Valley. *Mitekufat Haeven - Journal of the Israel Prehistoric Society* 45, 5-30.
- Ramsey, C.B., 2009. Bayesian analysis of radiocarbon dates. *Radiocarbon* 51, 337-360.
- Reimer, P.J., Bard, E., Bayliss, A., Beck, J.W., Blackwell, P.G., Ramsey, C.B., Buck, C.E., Cheng, H., Edwards, R.L., Friedrich, M., 2013. IntCal13 and Marine13 radiocarbon age calibration curves 0–50,000 years cal BP. *Radiocarbon* 55, 1869-1887.
- Sharon, G., Feibel, C.S., Belitzky, S., Marder, O., Khalaily, H., Rabinovich, R., 2002a. 1999 Jordan River Drainage Project Damages Gesher Benot Ya'aqov: A Preliminary Study of the Archaeological and Geological Implications, in: Gal, Z. (Ed.), *Eretz Zafon - Studies in Galilean Archaeology*. Israel Antiquities Authority, Jerusalem, pp. 1-19.
- Sharon, G., Marder, O., Boaretto, E., 2002b. A Note on 14C Dates From the Epi-Paleolithic Site at Gesher Benot Ya'aqov. *Mitekufat Haeven - Journal of the Israel Prehistoric Society* 32, 5-15.

Appendix 1



Excavation Daily Page 2017

Date: _____ / 9 / 2017
 Excavator: _____
 Area: _____
 Square _____
 Layer: _____



Example – Square L150-d Find Coordinates

		SubSq. a	SubSq. b	SubSq. c	SubSq. d	Buckets
Spit #1	Z- start					
	Z - end					
Description & Remarks:						
		SubSq. a	SubSq. b	SubSq. c	SubSq. d	Buckets
Spit #2	Z- start					
	Z - end					
Description & Remarks:						
General bag – date – Square – Sub-Square – Layer – Level Top – Level bottom – Excavator Name – type of find: Flint – Basalt - Limestone – Charcoal – Bone – Wood - Other						

Appendix 2

JRD: Molluscs from the archaeological levels: A preliminary analysis

Daniella E. Bar-Yosef Mayer

The Steinhardt Museum of Natural History, Tel Aviv University. baryosef@tauex.tau.ac.il

At JRD, two teams are studying the molluscan remains: One, headed by S. Mischke, studies the environmental conditions at the site with an emphasis on the levels without (in between) evidence for human occupation. The second team studies the molluscs at the site from the occupational levels, with its main goal being to explore the possibility that the site was a shell midden, while exploring the conditions during these periods.

This short report presents preliminary results from this analysis. Seven samples were collected by the excavators, representing seven different layers. All contained untreated sediments with a similar volume of a medium-sized ziplock bag. The content of the bags was picked by a student using tweezers, and shells were separated morphologically.

A total of 14053 were sorted. This represents the number of individual specimens (NISP) counted, including fragments and broken shells. The samples consist mostly of small gastropods and bivalves from the sediments of former Lake Hula, now situated on the banks of the River Jordan. At this time the samples have only been identified at genus level; however, the next step will be to identify the shells at species level. Because our preliminary analysis suggests that some of the species are no longer living in the region today, this process will take time.

The following table summarizes the preliminary counts:

	17#1; layer 3a	17#2; layer 3a?	17#3; layer 3c	layer 4a	#4; layer 4b	17#5; layer 5	17#6; above layer 5	Total by genus
<i>Theodoxus michonii</i>	32	81	40	110	127	74	162	626
<i>Valvata</i> and <i>Gyraulus</i>	0	0	0	129	122	62	194	507
<i>Heleobia</i> spp.	47	0	0			734	2497	3278
<i>Bithynia</i> spp.	0	0	0	1653	142	103	692	2590
<i>Melanopsis</i> spp.	221	384	125	3418	399	159	366	5072
<i>Unio terminalis</i>	563	79	80	405	145	183	20	1475
<i>Corbicula</i> spp.	53	120		0	0	0	0	173
<i>Pisidium</i> spp.	39	0	26	55	57	7	148	332
Total by layer	955	664	271	5770	992	1322	4079	14053

Acknowledgements: We are grateful to Henk K. Mienis for assistance with shell taxonomic identifications